CONFIDENTIAL

NACA

RESEARCH MEMORANDUM

FLIGHT AND PREFLIGHT EVALUATION OF AN AUTOMATIC

THRUST-COEFFICIENT CONTROL SYSTEM IN

A TWIN-ENGINE RAM-JET MISSILE

By H. Rudolph Dettwyler and Otto F. Trout, Jr.

Langley Aeronautical Laboratory
Langley Field, Va.

NATIONAL ADVISORY COMMITTEE
FOR AERONAUTICS
WASHINGTON
January 22, 1954

CONFIDENTIAL

Classification cancelled (or changed to ~~Unclassified~~)

By Authority of ~~NASA Tech Pub Announcement #3~~
(OFFICER AUTHORIZED TO CHANGE)

By.... ~~4 Feb 59~~

~~(GRADE OF OFFICER MAKING CHANGE)~~

~~5 March 59~~
DATE

NATIONAL ADVISORY COMMITTEE FOR AERONAUTICS

RESEARCH MEMORANDUM

FLIGHT AND PREFLIGHT EVALUATION OF AN AUTOMATIC

THRUST-COEFFICIENT CONTROL SYSTEM IN

A TWIN-ENGINE RAM-JET MISSILE

By H. Rudolph Dettwyler and Otto F. Trout, Jr.

SUMMARY

A flight and preflight evaluation has been made of an automatic thrust-coefficient control system in a twin-engine ram-jet missile. A flicker-type single-loop servocontrol system, which controls ram-jet diffuser recovery through the use of a fuel regulator, is shown to be a simple and workable scheme of controlling ram-jet thrust coefficients.

Preflight tests at a Mach number of 1.84 indicate the system to be stable and capable of maintaining the engine thrust coefficient between 0.725 and 0.748 at a particular control pressure-ratio setting. Flight data showed that the thrust coefficient varied from 0.56 to 0.68 over a range of Mach number. Combustor blowout occurred in flight at a free-stream Mach number of 3.06 and an altitude of 67,950 feet.

INTRODUCTION

The primary function of a ram-jet thrust control system is to maintain a set of conditions by supplying the proper fuel flow to the engines. Such a regulator should possess the qualities of simplicity, reliability, and capability of maintaining conditions within the operating limits of the engines. In particular, diffuser instability should be avoided and the rich and lean fuel-air ratio limits of the combustor should not be exceeded.

In the past, several methods of thrust regulation have been suggested. The most common of these is a scheme for direct metering of the fuel-air ratio. Such a system can become complex because compensating devices for changes in free-stream temperature, pressure, and Mach number are necessary. In addition, diffuser stability limits are not directly avoidable. Ram-jet control systems may also be operated by use of diffuser pressure

recovery. In reference 1 a scheme of this type is proposed, in which the fuel control system essentially maintains a constant engine thrust coefficient by controlling the ram-jet-diffuser pressure recovery. Such a system is not affected by the changing free-stream temperature and pressures under which the engine is required to operate. This ram-jet thrust control system was conceived because ram-jet thrust is directly related to combustor-entrance total pressure. Reference 2 presents analytical and experimental analyses of the relationship between jet thrust and diffuser performance.

The purpose of this paper is to describe the thrust-coefficient control system and present data from both flight and preflight tests. Performance and operating characteristics of the regulator are presented for a range of Mach numbers and altitudes encountered by the test vehicle during free flight. The design, development, and evaluation of a closed-loop thrust-coefficient control system, utilizing diffuser pressure recoveries, has been undertaken by the Langley Pilotless Aircraft Research Division in conjunction with the ram-jet flight research program.

The NACA twin-engine test vehicle described in references 3 and 4 has been found satisfactory for this program, having the advantages of small size, accessibility, stable combustion to an altitude of over 60,000 feet, and a self-pressurized fuel system.

SYMBOLS

A   area, sq ft

a   servo damping-to-inertia ratio, per second

B   dimensionless amplitude factor

C_D external drag coefficient, based on $A_2 = 0.462$ sq ft

C_T thrust coefficient, based on combustion-chamber area of both engines, 0.462 sq ft

g   acceleration due to gravity, 32.2 ft/sec^2

H   total pressure, lb/sq in. abs

H_n pressure behind normal shock, lb/sq in. abs

H_n/H_2 control pressure ratio

H_2/H_0 diffuser recovery

M   Mach number

P   static pressure, lb/sq in. abs

P_x control static pressure ahead of sonic orifice

ΔP control pressure differential, $H_n - P_x$

T_0 ·ambient static temperature, $^\circ F$ abs

τ average time lag between instantaneous control signal and control differential pressure reversal, sec

Subscripts:

0   free stream

1   diffuser inlet

2   diffuser exit, combustion-chamber entrance

3   combustion-chamber exit

4   nozzle exit

APPARATUS

Test Vehicle

The test vehicle with twin ram-jet engines installed on the tail surfaces is shown in figure 1(a). The vehicle weighed 258 pounds including 25 pounds of gaseous ethylene fuel. Except for an automatic fuel control system, the vehicle was similar to that discussed in references 3 and 4. The test vehicle and booster are shown in the launching position in figure 1(b).

In order to prevent the test vehicle from going beyond an allowable test range, a set of retractable canard surfaces was installed in the nose section. Figure 1(c) shows the canards in the extended position. These canards remained within the nose until 70 seconds after take-off at which time they were extended by the opening of an electrically actuated lock. The canards were designed with sufficient area to make the vehicle aerodynamically unstable.

Ram-Jet Engines

Two identical ram-jet engines mounted on the horizontal tail surfaces were 6.6 inches in diameter, 52.30 inches long, and weighed 36.5 pounds each. The inlets, designed for $M_0 = 2.15$, and the burners are identical to those described in references 3 and 4. A sectional view of the engine is presented in figure 2. A supersonic exit nozzle with a contraction and expansion ratio of 0.78 and 0.76, respectively, was used.

Thrust-Coefficient Control System

The basic principles of the automatic control system have previously been described for ram-jet applications in reference 1. The system utilizes an on-off type of servocontrol which has residual oscillations during steady-state operation. A schematic diagram of the control system is shown in figure 3. By using the ram-jet diffuser-exit total pressure H_2 and measured pitot stagnation pressure H_n relationship, the fuel-control valve regulates to a constant engine thrust coefficient at any given flight Mach number. This thrust-coefficient control is accomplished by maintaining a desired ratio between the measured pitot stagnation pressure H_n and the ram-jet diffuser-exit total pressure H_2.

In order to operate the engine at a pressure greater than normal-shock pressure recoveries, a sonic bleed orifice was used on the diffuser pressure line. This sonic orifice was so adjusted that an average ratio of 0.925 was maintained between the diffuser total pressure rake and the static pressure ahead of the sonic orifice. In making this adjustment the line losses between the rake and bleed orifice were taken into account. The control pressure ratio H_n/H_2, then, fixed the operating engine diffuser recovery H_2/H_0 which in turn established the thrust coefficient at a given Mach number.

The system uses the measured diffuser-exit pressure from only one engine.

A sensitive zero-differential pressure switch is used to compare the measured H_n and P_x. Figure 4 shows a schematic drawing of the zero-differential pressure switch. The body of the switch was constructed of aluminum. A sensitive metallic diaphragm was used to make an electrical contact. When the ratio of P_x/H_n is greater than 1, a signal is given to the relay which in turn controls the servomotor. Then the motor rotates the sleeve valve to decrease the free port area to each engine for lower fuel flows. The reverse sequence occurs when the ratio P_x/H_n is less than the 1.

With this flicker-type system, no null point exists; therefore, the servomotor will continuously run in one direction or the other and produces residual hunting.

Fuel Control Valve

The fuel-control-valve assembly serves four functions:

(1) As a quick-opening, electric-squid-operated, bypass starting valve

(2) As a quick-opening, squib-operated, main flow port

(3) As a variable flow control valve for regulating engine fuel flow

(4) As a distributing manifold to supply equal fuel rates to each engine

The complete valve assembly with motor drive weighed 7 pounds. Photographs of the assembled and disassembled valve are shown as figure 5.

The quick-opening starting valve supplies a reduced fuel flow to each engine during the ram-jet ignition period. This reduced fuel flow is necessary, because the engines, which are ignited during the vehicle boost period, will not ignite reliably at the normal operating fuel rates.

The main port opens shortly after the starting bypass port opens; a condition which allows the engines to operate at the normal-flow rate determined by the open area of the variable fuel control valve.

The bypass and main fuel ports are opened at predetermined intervals by electric delay squibs fired at zero time on the launcher after the booster is fired. Both of these valves are actuated by the pressure from the operative squib acting on a piston attached to the valve.

The motor-driven rotary sleeve valve was designed to produce a 32.5 percent change in open area per second. Separate ports of equal area provide each engine with equal fuel rates.

Booster

A sketch of the multirocket-booster assembly is presented in figure 6. Three JATO 3.5 ES-5700 rocket motors each with a total impulse of 18,000 pound-seconds, were mounted in a cluster and fired simultaneously. The forward ends of the rocket motors were mounted in a magnesium casting,

which also served as a coupling to the test vehicle. The rearward ends
of the rockets were joined by the fin structure. Three booster fins,
each with an exposed area of 3 square.feet, were spaced 120° apart.

Preflight Jet Facility

The preflight tests of the twin ram-jet engines were conducted in
the 12- by 12-inch, M = 1.84 preflight jet at the Langley Pilotless
Aircraft Research Station at Wallops Island, Va. Sea-level tests and
simulated pressure-altitude conditions up to approximately 8,000 feet
were performed by controlling the tunnel pressure. Figure 7 shows the
twin-engine installation in the M = 1.84 preflight jet.

INSTRUMENTATION AND METHODS

Preflight Measurements

The internal ram-jet pressures measured in each engine (fig. 2) were
the diffuser-exit total pressure, the combustion-chamber-exit static pres-
sure, and the fuel injection pressure. The diffuser-exit total pressure
was measured by a manifold rake which was perpendicular to the plane of
the innerbody strut. The sonic bleed orifice was attached to the line
which connected one side of the diffuser pressure switch and the dif-
fuser rake from one engine (fig. 3). The opposite side of the pressure
switch was connected to a probe mounted in the jet stream between the two
inlets. Fuel flow control characteristics were evaluated by recording
the fuel tank pressure, injection pressure, control pressure differen-
tial $H_n - P_x$, pressure-switch signal, and valve position compared on a
time basis with internal engine characteristics. Both engines were mounted
on a strain-gage beam balance which recorded the thrust in excess of drag
during combustion. From these measured quantities, the engine thrust
coefficients, air-mass flows, and total pressure recoveries were deter-
mined in the same manner as that reported in reference 5.

Prior to flight testing, the control system was evaluated with the
actual test-vehicle engines mounted in the 12- by 12-inch, M = 1.84 pre-
flight jet as shown in figure 7. A preliminary study of the expected
flight conditions showed that the minimum speed expected with the use of
the multirocket booster was M = 1.90. The system was therefore tested
at M = 1.84 in order to impose an even more critical pressure-recovery
condition for the control tests. The fuel-control equipment from the
model was mounted near the engines, out of the jet airstream. Fuel lines
and control-pressure lines were made to approximate the length and size
of those in the test vehicle.

Three different tests were conducted at $M = 1.84$. The first test of the control system used constant fuel pressure and density along with constant tunnel free-stream static pressure. The second test was conducted with constant fuel pressure and density, with a variation of tunnel free-stream static pressure from 14.8 to 12.5 lb/sq in. abs. In the third test, a fuel tank of equal capacity to that of the flight tank was filled and used to supply fuel to the engines during the test. The tunnel free-stream static pressure was decreased in such a manner as to approximate the static pressure expected in the early part of the flight trajectory. A maximum pressure altitude of 8,000 feet was simulated in this manner. Component parts of the fuel control system were made to operate in the same sequence and under conditions approximating those of the actual flight trajectory.

Ram-jet ignition was achieved through the use of reduced fuel flow and a combustor restriction as reported in reference 4.

Flight Instrumentation

The flight path of the test vehicle was obtained by NACA modified SCR 584 tracking radar during the first 40 seconds of flight. Continuous-wave Doppler radar near the launching site was used to measure velocity for the first 18 seconds of the flight.

An NACA nine-channel telemeter transmitted measurements of pitot stagnation pressure, longitudinal acceleration, total pressure and static pressure in the left engine, and control pressure differential $\Delta P = H_n - P_x$ in the right engine. The fuel-injection-pressure measurements of the controlled engine and the differential pressure-switch signal were also telemetered. In addition, two low-range instruments were used to measure the left-engine total pressure and the pitot stagnation pressure in the high-altitude-flight region.

Balloons carrying radiosondes were released before and after take-off in order to obtain atmospheric conditions which are plotted in figure 8.

Description of Flight Test

The flight test was conducted at the Langley Pilotless Aircraft Research Station at Wallops Island, Va. The test vehicle was launched at a 67° angle of elevation and was accelerated to $M = 2.07$ by the booster. Fuel flow was started at 1 second after take-off. Ignition of the engines occurred at 2.28 and 2.36 seconds after take-off, corresponding to $M = 1.67$ and $M = 1.75$, respectively. Booster separation occurred at 3.10 seconds, and during the next 29 seconds the engines operated to an altitude of 67,950 feet. Figure 9 presents the flight trajectory up

to 100 seconds. A maximum Mach number of 3.14 was attained (fig. 10) at 29.00 seconds after take-off at an altitude of 60,700 feet.

Combustion ceased at 31.28 and 32.24 seconds after take-off at M = 3.06 for the left and right engines, respectively. During the period of 4 to 14 seconds, the fuel regulator was effective in controlling the thrust coefficient in accordance with the thrust control balance. After this period, no signals from the pressure switch or movement of the control valve were shown on the records. However, the thrust coefficient remained approximately at the required value during the period from 14 to 32 seconds.

During the burning phase of the flight, a zero-lift trajectory was maintained. After combustor blowout, the vehicle coasted to a computed peak altitude of 135,000 feet at a computed range of 32 miles (fig. 9). During the coasting period, at approximately 70 seconds, the canard fins were extended. Flight trajectory was computed on a zero-lift basis to 100 seconds based on the accelerometer data. After 100 seconds, the accelerometer data became erratic, and because there was no basis for computing the position of the test vehicle after this period, no further data are presented. Telemeter signals were recorded, however, until the test vehicle returned to earth which occurred $8\frac{1}{2}$ minutes after take-off.

RESULTS AND DISCUSSION

Preflight Tests

The performance of a supersonic ram-jet engine can be evaluated by utilizing the relationship of the engine thrust coefficient, diffuser recovery, and combustion-chamber static-pressure ratio at any free-stream Mach number condition. The basic principle of the thrust-coefficient control system tested is based on the fact that H_2/H_0 and C_T are directly related regardless of free-stream temperatures and pressures. Figure 11 presents the experimental results of the twin ram-jet engines at M = 1.84 free-jet conditions in terms of internal pressure ratios and thrust coefficient for $T_0 = 405$ and $382°$ F abs. These data show a linear relationship up to diffuser instability. It is apparent that, by controlling the engine diffuser recovery, the thrust coefficient is controlled.

The first preflight test was conducted under steady-state conditions where the free-stream static pressure P_0 and fuel pressure and density were constant. This condition also served the purpose of calibrating the control pressure sonic bleed orifice to give the proper pressure ratio

and thrust coefficient. When the sonic orifice was sized the line pressure losses up to the point of its attachment were taken into account. Figure 12(a) presents a typical operating cycle for the steady-state conditions where $P_0 = 14.80$ lb/sq in. abs and $T_0 = 386^\circ$ F abs.

The data show that an average diffuser recovery H_2/H_0 of 0.855 with variations from 0.840 to 0.865 and an average thrust coefficient $C_T = 0.727$ with variations from 0.715 to 0.740 were maintained.

The control differential pressure $H_n - P_x$ which varied from 0.50 lb/sq in. to -0.50 lb/sq in. produced a signal for the fuel valve to close when the pressure changed from plus to minus and vice versa. A steady-state average period of oscillation of 1.33 seconds and a control pressure amplitude of ± 0.50 lb/sq in. is indicated in figure 12(a).

Figure 12(b) presents the results obtained with decreasing free-stream static pressure and constant fuel pressure. These results show that the diffuser recovery varied between 0.865 and 0.845 and the thrust coefficient ranged from 0.725 to 0.748, whereas the free-stream static pressure P_0 varied from 13.65 to 12.5 lb/sq in. abs in a period of 2.4 seconds.

The results of the preflight test simulating the early part of the trajectory are presented in figure 13. This test was conducted with a fuel system similar to that used in the flight test by the use of a fuel tank of equal capacity. The tunnel free-stream static pressure P_0 varied from 14.8 to 11.1 lb/sq in. abs in a period of 9 seconds. When the main fuel port opened, the control pressure switch gave an open signal because the valve was not supplying sufficient fuel flow. Between 3 and 5 seconds, at a free-stream static pressure of 14.15 lb/sq in. abs, the system began to regulate. Automatic control was maintained to approximately 13.2 lb/sq in. abs at which time the flow control valve indicated wide open because of insufficient fuel pressure in the tank. During the control period, the fuel injection pressure remained nearly constant even though the tank pressure was decreasing; however, after the valve reached maximum open area, the injection pressure decreased. In the control region, an average diffuser recovery of 0.850 and a thrust coefficient of 0.725 was maintained and the average control pressure ratio H_n/H_2 was 0.925.

A theoretical curve of diffuser recovery plotted against flight Mach number is shown in figure 14 for different control pressure ratios, H_n/H_2. The experimental point obtained from the preflight tests is indicated and shown to be below the diffuser-instability limits.

The curves in figure 14 also indicate that at $M = 1.84$, it would be impossible to operate the engines without encountering diffuser instability

at a control pressure ratio of less than 0.910; however, the selected control pressure ratio of 0.925 is shown to be entirely satisfactory over a Mach number range of 1.84 to 3.2. At the expected minimum boost velocity M = 1.9, a 4-percent margin in diffuser recovery exists. The diffuser-instability curve was obtained from experimental valves of reference 5. The theoretical curves of figure 14 were obtained by the methods presented in reference 2. The ram-jet diffuser must operate supercritically in order for this type of control system to be effective. Additional limitations and modifications of this control system are discussed in detail in reference 1.

Flight Tests

The flight path of the test vehicle was obtained from tracking radar up to 40 seconds and extended to 100 seconds after take-off by means of accelerometer data. Flight Mach number plotted against time, as presented in figure 10, was obtained by three methods: (1) from CW Doppler radar data extended by integration of the accelerometer data, (2) by use of measured pitot stagnation pressure and atmospheric data, and (3) by integration of the accelerometer data. Figure 10 also presents engine air-mass flow plotted against time, calculated from Mach number, atmospheric data, and inlet mass-flow data by methods presented in reference 5. The ram-jet engines sustained combustion with air rates varying from 14.85 to 1.60 pounds of air per second per engine.

Figure 15 presents values of measured longitudinal acceleration plotted against time, for the ram-jet powered part of the flight. The test vehicle maintained positive acceleration as long as both engines maintained combustion.

A maximum thrust coefficient of 0.69 and a minimum of 0.56 were obtained for the flight, as shown in figure 16. A higher thrust coefficient was obtained at M = 1.84 in the preflight tests because of the characteristics of the control system below design Mach number of the inlet. Reasons for this higher thrust coefficient are presented in detail in reference 1. A fuel-air ratio of 0.056 at blowout was calculated for the measured thrust (from acceleration and drag data) for an assumed combustion efficiency of 80 percent. No measurements were made of fuel rate in flight. A total impulse of 23,176 lb-sec was obtained between 4 and 31 seconds after take-off.

Figures 17 and 18 show that the greatest variation in C_T occurred in the early part of the flight, where air and fuel densities were the greatest. For the ram-jet powered part of the flight, the thrust coefficient was well in excess of the drag coefficient (fig. 17).

Figure 18 presents thrust coefficient, differential pressure, diffuser recovery, free-stream Mach number, free-stream static pressure, and the control signal to the flow control valve plotted against time for a part of the flight test. Examination of these data shows that the period of oscillation of the system was approximately three times that encountered in the preflight tests, whereas the control-differential-amplitude variation was about twice. A pressure-switch sensitivity of ±0.25 lb/sq in. was recorded during the flight.

It can be seen in figure 18 that the engine diffuser recovery is decreasing with time, whereas the thrust coefficient is relatively constant. This effect is caused by increasing flight Mach number during the period shown. Figure 14 showed the expected and actual recoveries as a function of the flight Mach number. During the last part of the flight, in the region from $M = 2.95$ to $M = 3.1$, the diffuser recovery was essentially approaching normal shock recoveries $\left(H_n/H_2 = 1.0\right)$, a condition which indicates insufficient fuel flow.

An analysis of the flicker system, utilizing on-off signals, in steady-state operation shows that various time lags affect the period of oscillation and amplitude. Figure 19(a) presents the theoretical characteristics for such a system presented in this paper. The direct current motor has been represented by its characteristic damping-to-inertia ratio and the remainder of the system, such as pressure switch relay, valve, fuel flow response, and internal pressure-thrust lags, has been represented as one single time lag. The preflight data indicated this average system time lag to be 0.22 second. The method of analysis used is that presented in reference 6.

Inasmuch as the valve position was not available from flight measurements, figure 19(b) was prepared to show the relationship between control valve amplitude, in degrees, and control pressure amplitude. This relationship then allows the pressure-amplitude curve of figure 19(a) to be determined. It can be seen that a ratio of approximately $2°$ per lb/sq in. exists for the preflight test conditions. Good agreement exists between the analytical and experimental data.

Because the flight analysis indicates that the control system operated with a period of 4 seconds and an amplitude of 1 lb/sq in., the actual system time lag had to be greater than that measured in preflight tests. From the theoretical curve, these values of period and amplitude indicate an approximate time lag of 0.90 second. No explanation of this apparent increased time lag is known. Although the control-system time-lag characteristic differed in flight from that experienced in preflight tests, no harmful effects are noted on the operation and performance of the thrust-coefficient control system.

SUMMARY OF RESULTS

In this investigation of a ram-jet thrust-coefficient control system, a characteristic of which is residual oscillations in steady-state operation, the following facts were observed from preflight and flight tests.

(1) Satisfactory control-system performance was obtained during preflight tests. The diffuser total pressure was maintained within ±0.50 lb/sq in. during the tests.

(2) Satisfactory operation of the control system was obtained during flight for a period of 14 seconds. The diffuser-exit total pressure was maintained within ±1.0 lb/sq in. during this period. Although there was an increase in time lag and amplitude of the system, compared with preflight tests, no harmful effects resulted.

(3) Satisfactory operation of the differential pressure switch was obtained throughout the flight with a sensitivity of ±0.25 lb/sq in.

(4) During the flight, the engine thrust coefficient varied from 0.56 to 0.69. The ram-jet powered part of the flight covered an altitude range from near sea level to 67,950 feet and a Mach number range from 2.02 to 3.14.

(5) Ram-jet combustion ceased at a Mach number of 3.06 with an engine air-mass flow of 1.60 pounds per second at an altitude of 67,950 feet. A fuel-air ratio of 0.056 based on measured thrust and an assumed combustion efficiency of 80 percent were computed for these conditions. During the period from 4 to 31 seconds after take-off, a total impulse of 23,176 lb-sec was delivered by the two ram-jet engines.

Langley Aeronautical Laboratory,
    National Advisory Committee for Aeronautics,
        Langley Field, Va., October 28, 1953.

CONFIDENTIAL

REFERENCES

1. Faget, Maxime A.: A Proposed Ram-Jet Control System Operated by Use of Diffuser Pressure Recovery. NACA RM L52E05b, 1952.

2. Dettwyler, H. Rudolph, and Faget, Maxime A.: Engineering Method of Ram-Jet Thrust Determination Based on Experimentally Obtained Combustor Parameters. NACA RM L53E21, 1953.

3. Dettwyler, H. Rudolph, and Bond, Aleck C.: Flight Performance of a Twin-Engine Supersonic Ram Jet From 2,300 to 67,200 Feet Altitude. NACA RM L50L27, 1951.

4. Faget, Maxime A., and Dettwyler, H. Rudolph: Initial Flight Investigation of a Twin-Engine Supersonic Ram Jet. NACA RM L50H10, 1950.

5. Hinners, Arthur H., Jr., and Foland, Douglas H.: Preflight Tests and Flight Performance of a 6.5-Inch-Diameter Ram-Jet Engine. NACA RM L53H28, 1953.

6. Curfman, Howard J., Jr., and Gardner, William N.: Theoretical Analysis of the Motions of an Aircraft Stabilized in Roll by a Displacement-Response, Flicker-Type Automatic Pilot. NACA RM L8D19, 1948.
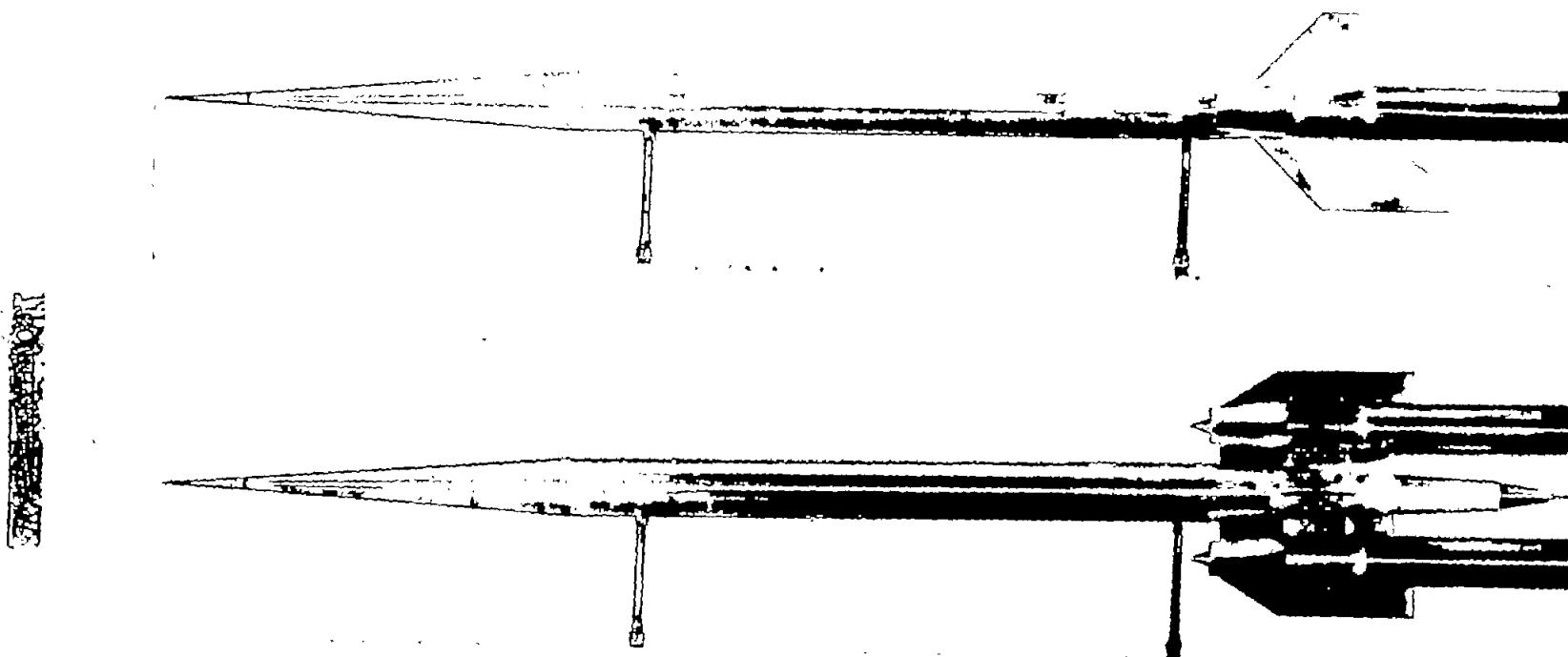
CONFIDENTIAL

L-82056

(a) Two views of flight test vehicle.

Figure 1.- Ram-jet test vehicle.
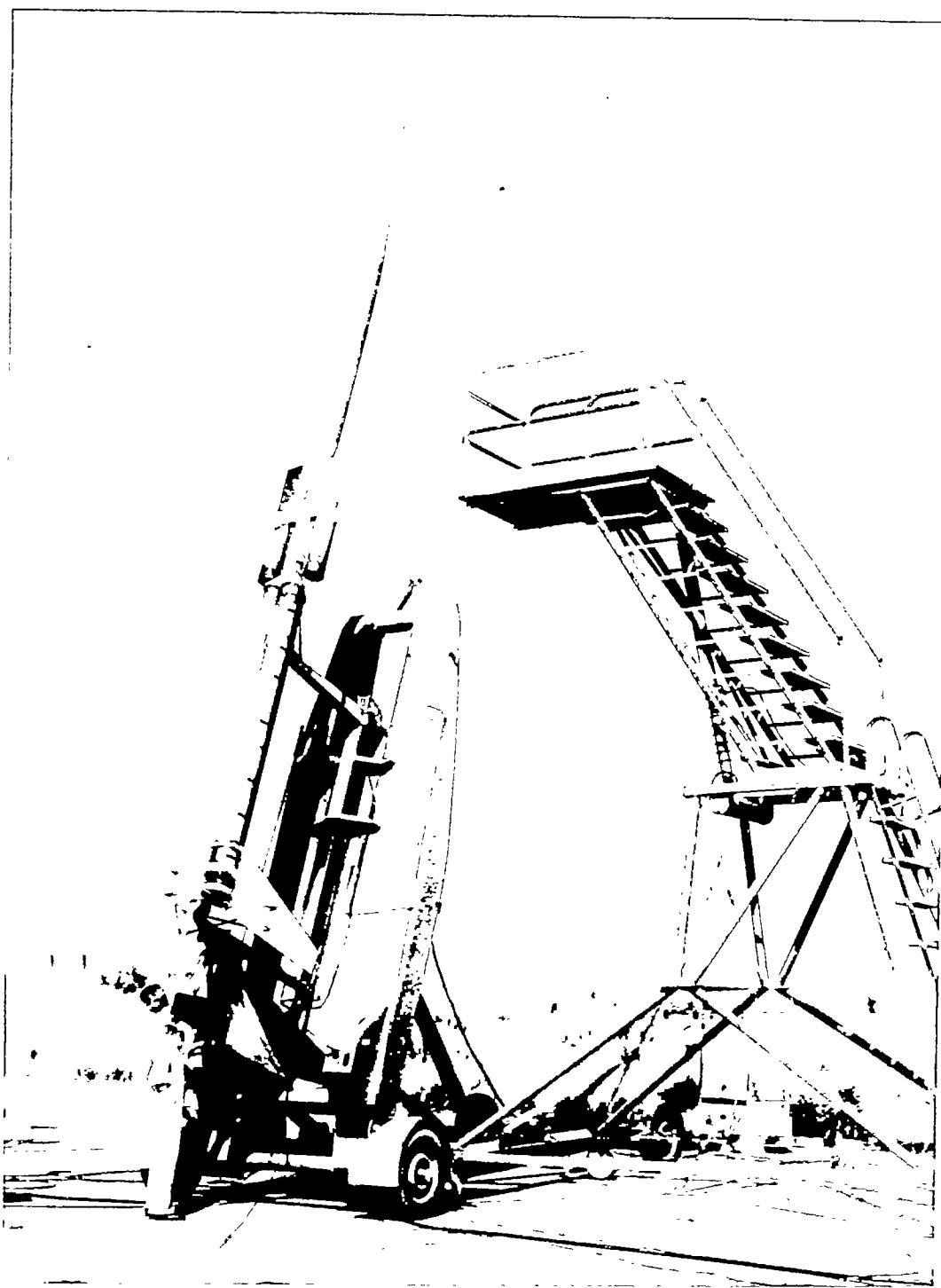
L-81006.1

(b) Test vehicle and booster on launcher.

Figure 1.- Continued.
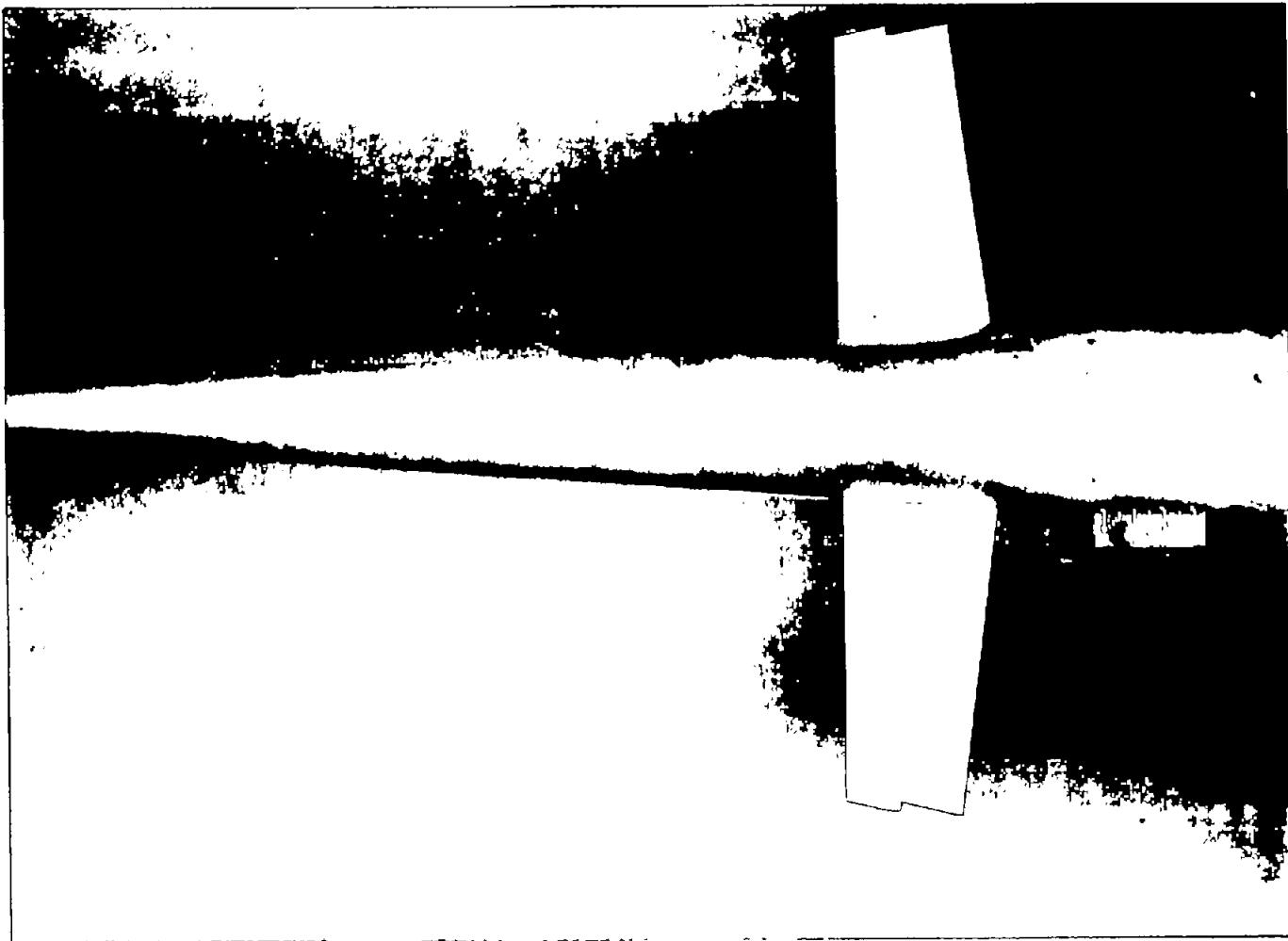
L-71876

(c) Canards in extended position.

Figure 1.- Concluded.

"CONFIDENTIAL"
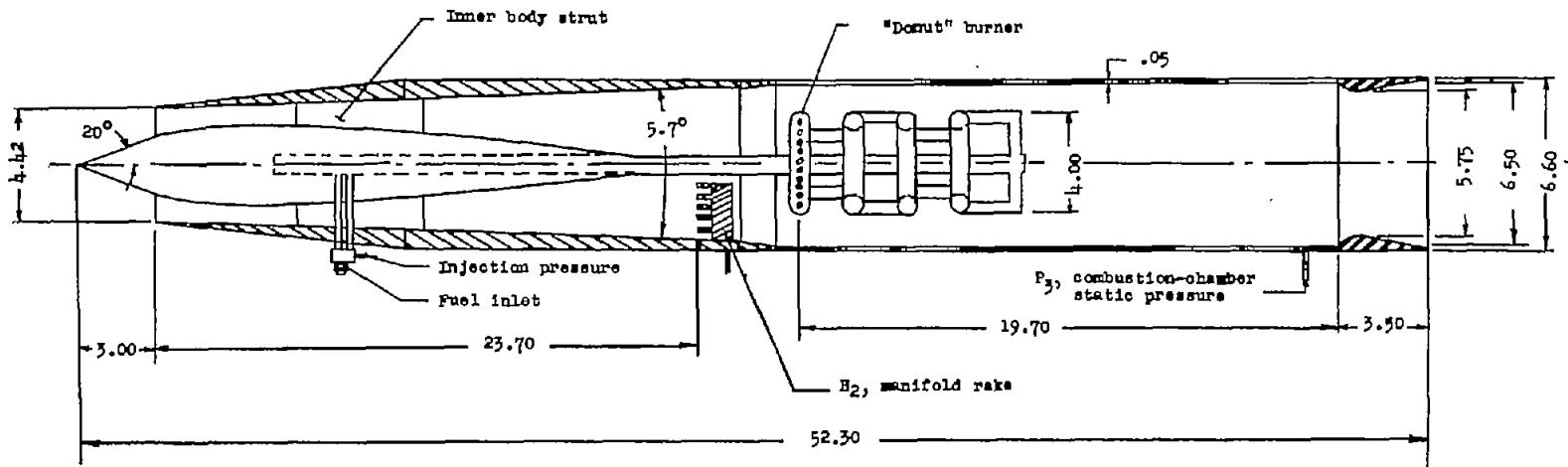
Figure 2.- Section view of ram-jet engine. All dimensions in inches.
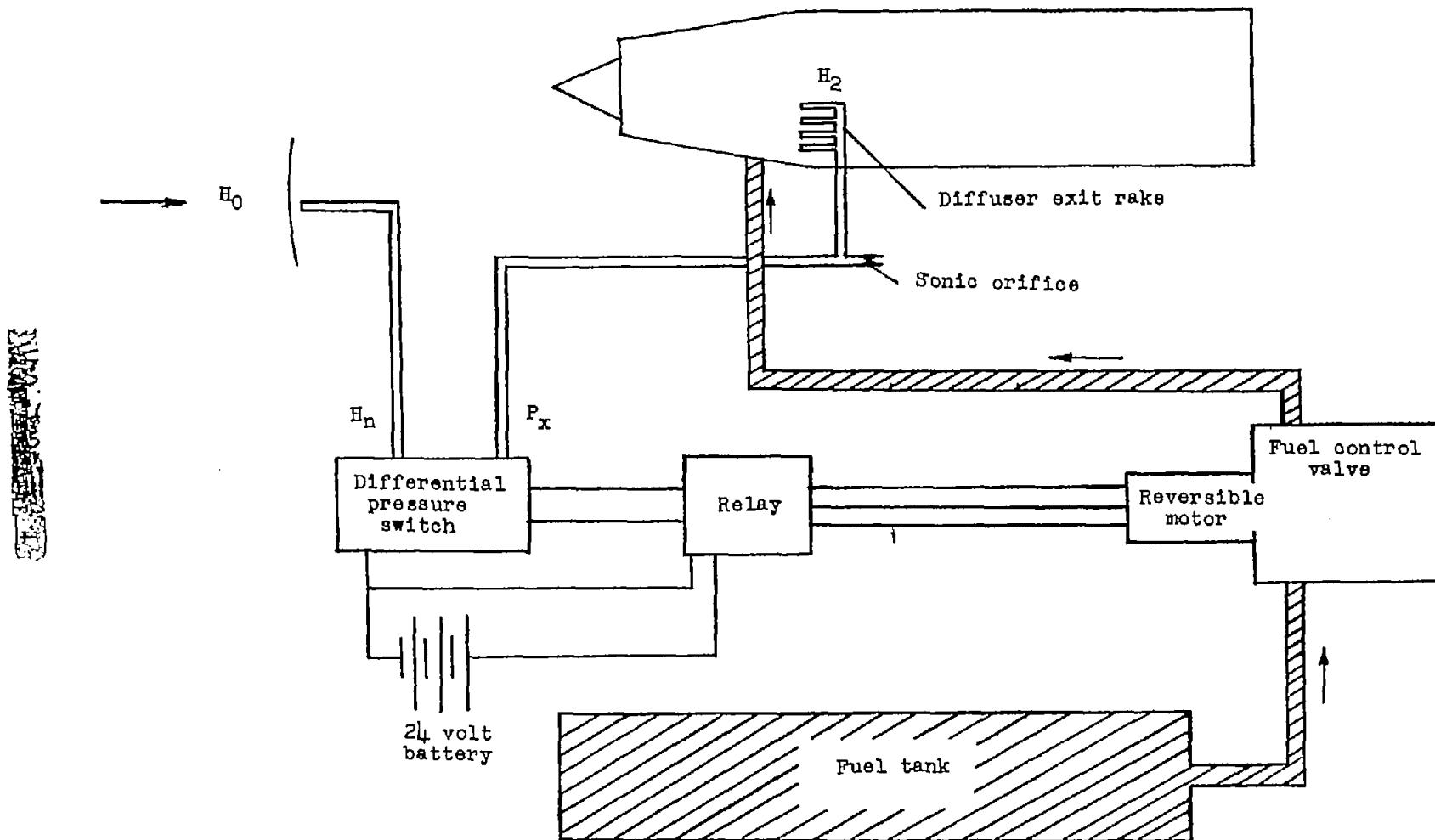
Figure 3.- Schematic diagram of automatic thrust-coefficient control system.

H_n

Silver contacts

Metal diaphragm

P_x

1.87 diam

1.50
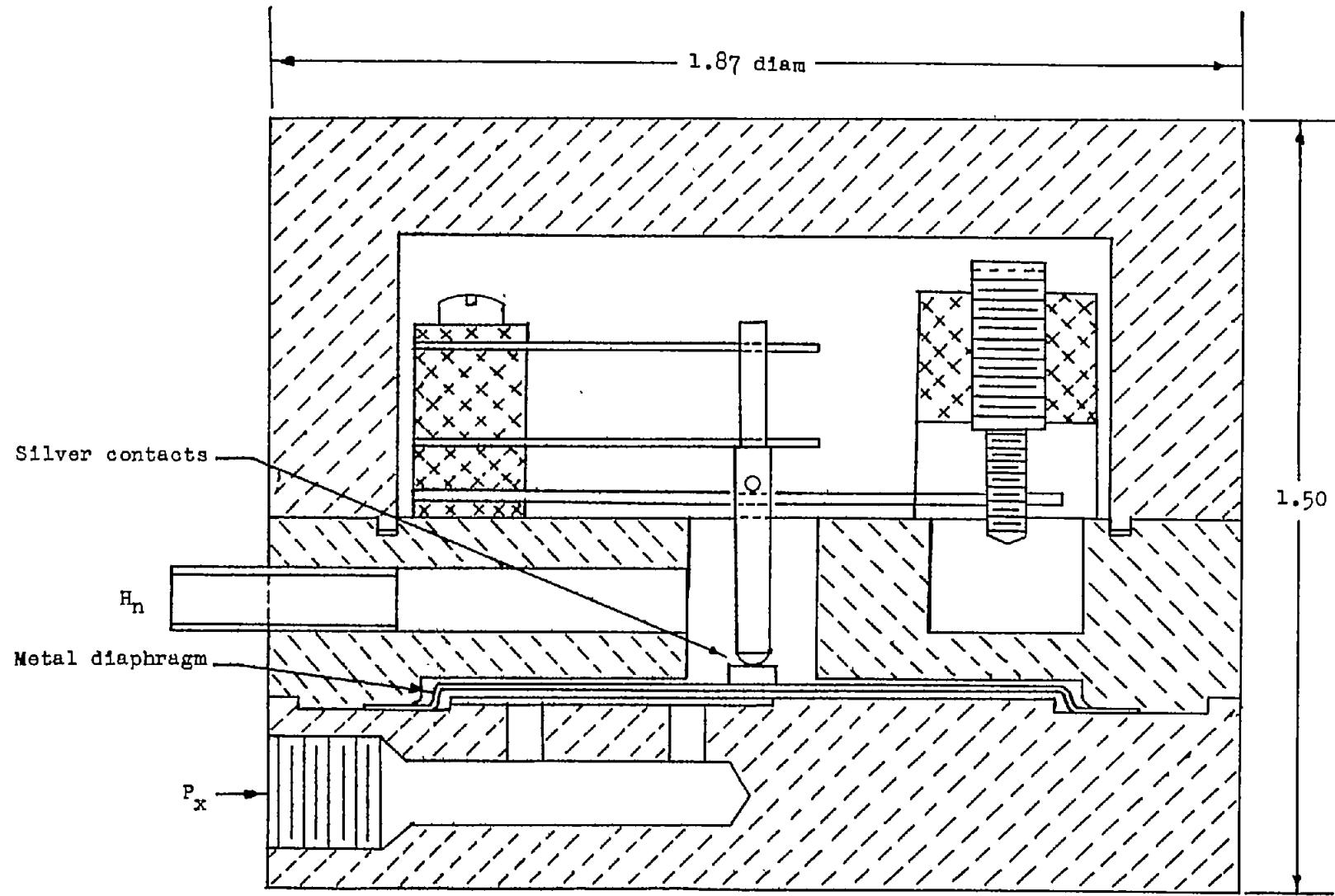
Figure 4.- Sketch of differential pressure switch.
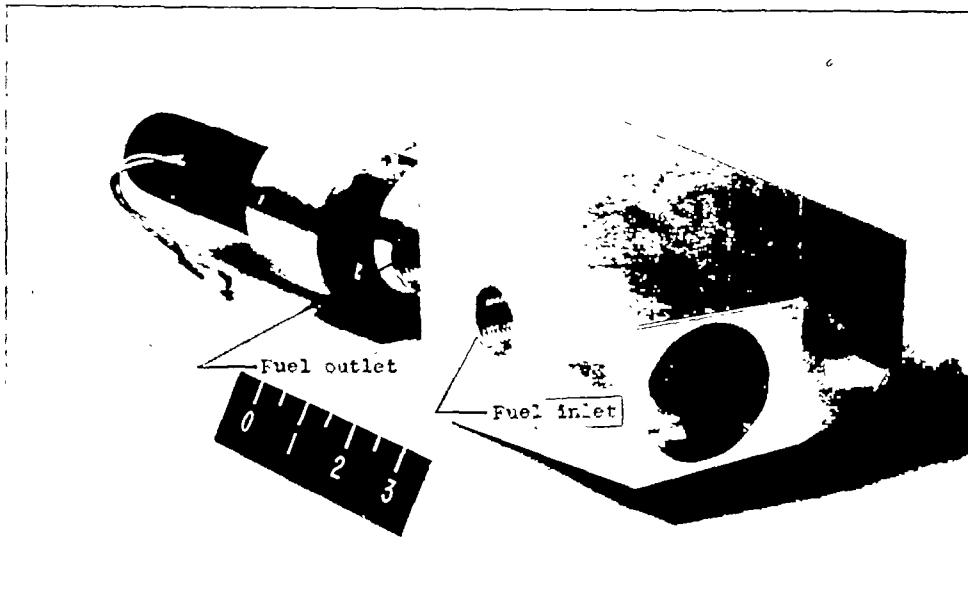
L-72394.1

(a) Completely assembled valve.
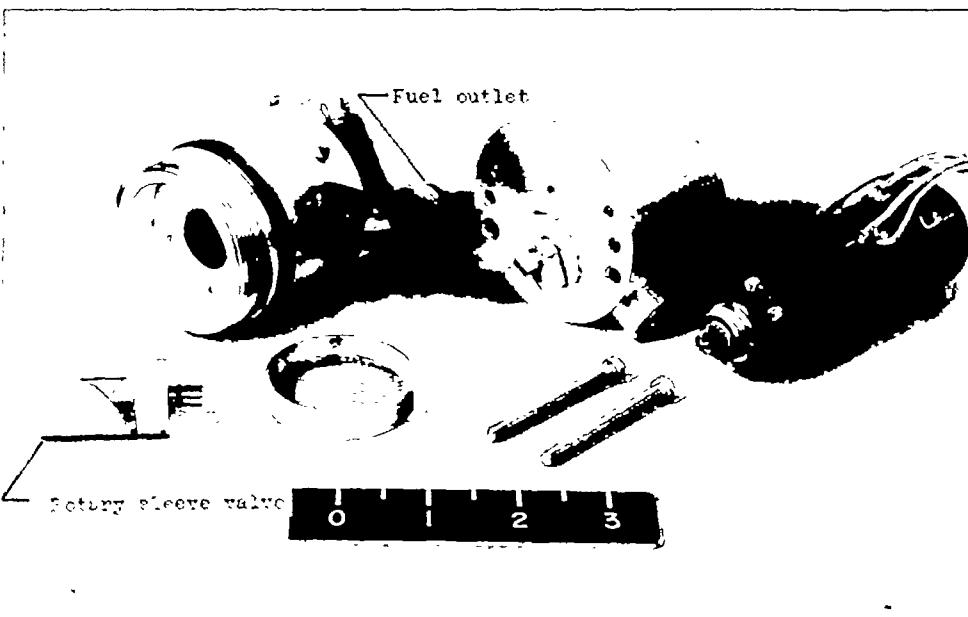
L-74942.1

(b) Breakdown of motor driven sleeve valve.

Figure 5.- Fuel control valve.

Squib ports

Fuel inlet

Main valve port

Starting valve port

Piston

Piston

Starting valve orifice

Valve body

0   1   2   3
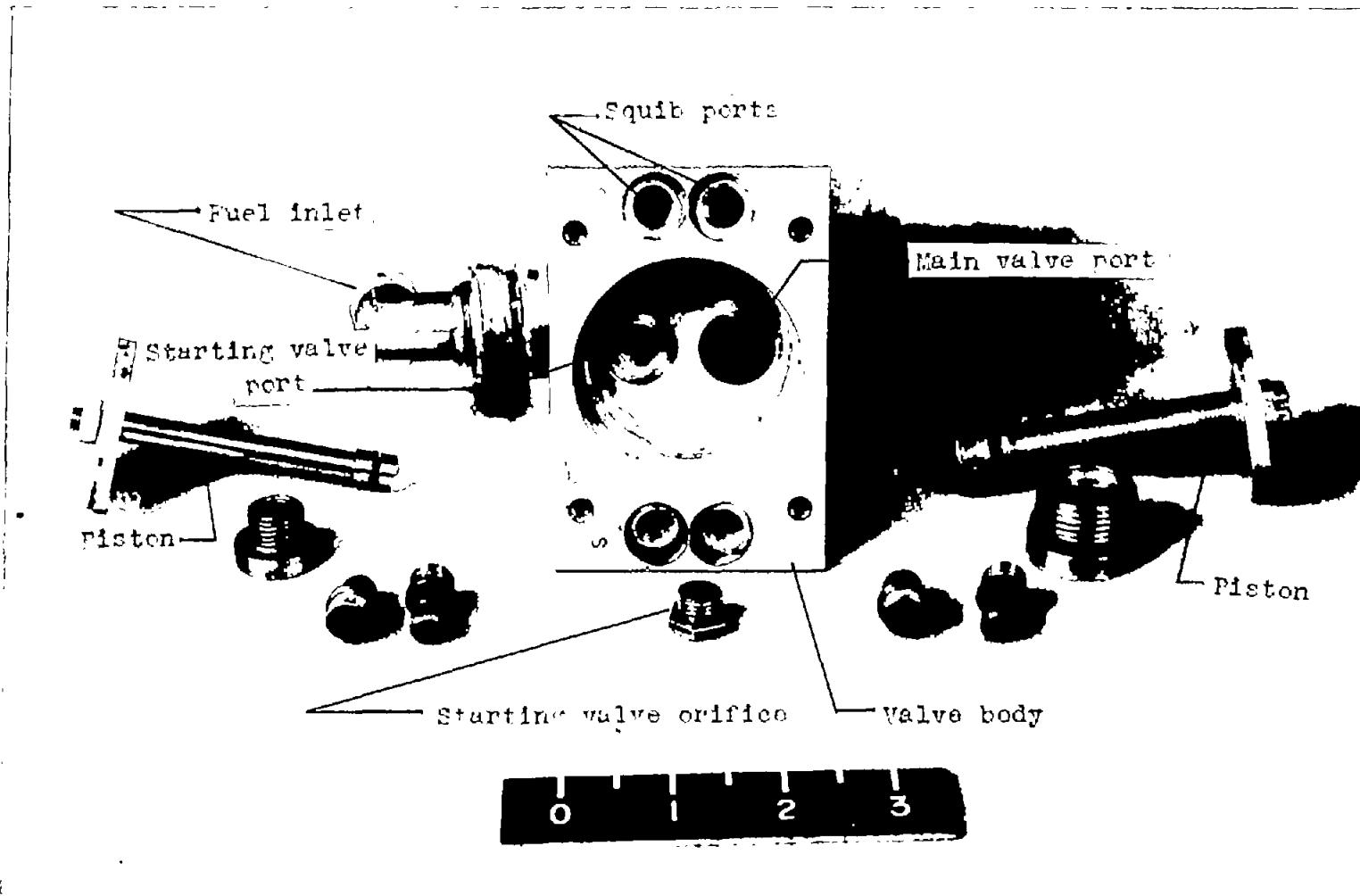
L-74943.1

(c) Breakdown of squib-operated valves.

Figure 5.- Concluded.
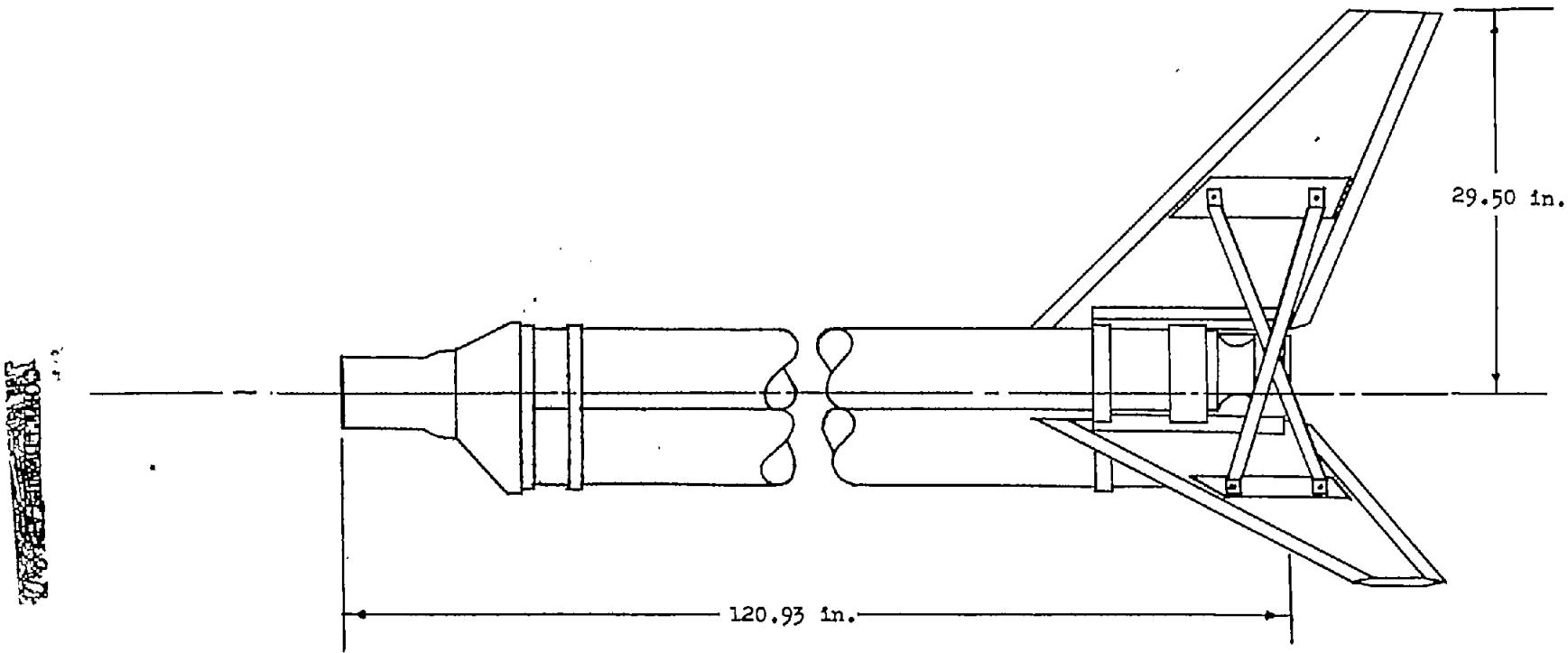
Empty weight, 212 lb
Loaded weight, 510 lb

Fin data
Area, 3 sq ft per panel
Tip chord, 7.375 in.
Root chord, 22.00 in.
Taper ratio, 0.333
Leading edge angle, 45°

Figure 6.- Sketch of test vehicle booster.
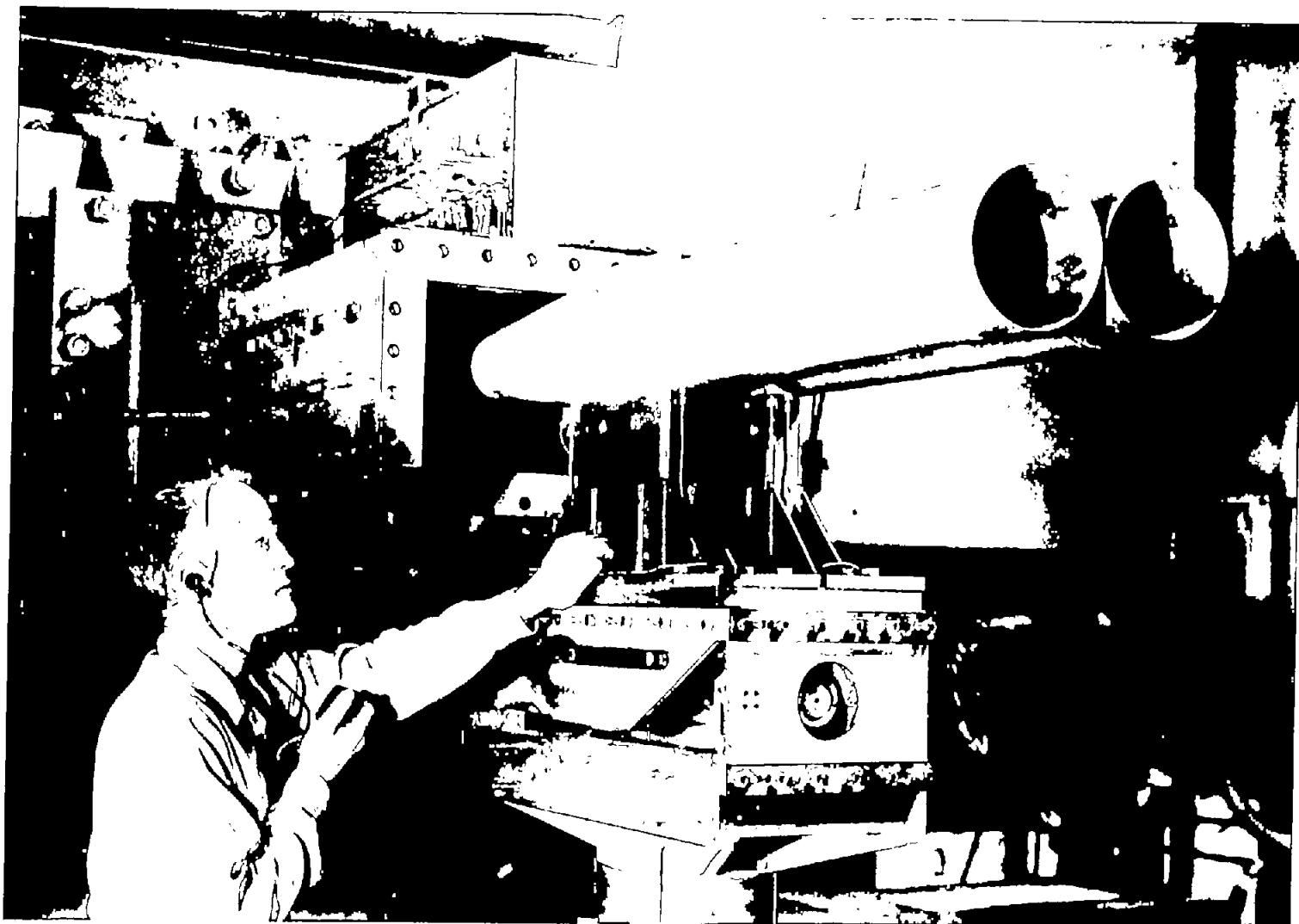
L-70450

Figure 7.- Preflight test setup in M = 1.84 free jet.
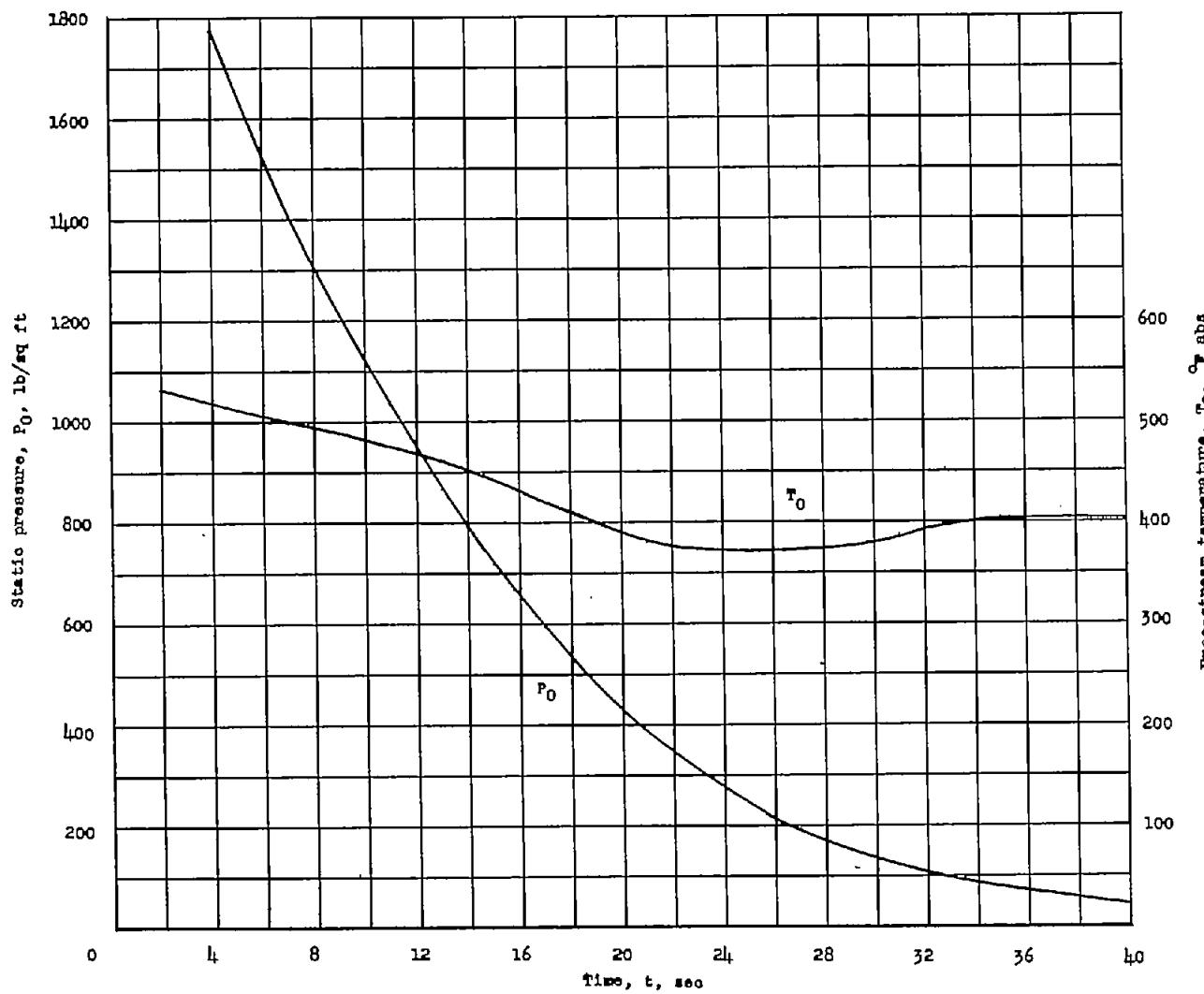
Figure 8.- Free-stream static pressure and temperature plotted against time for the flight test.
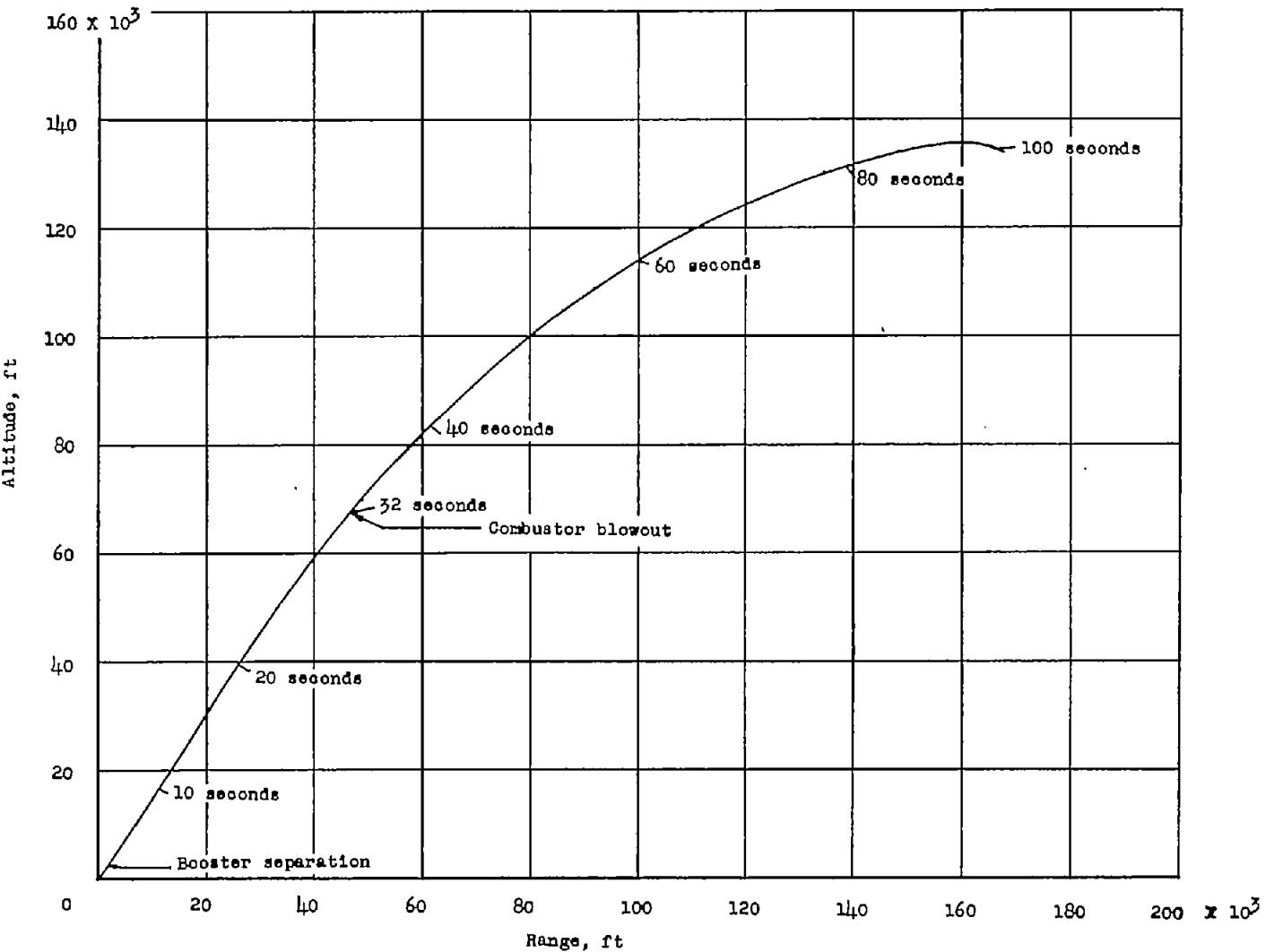
Figure 9.- Altitude plotted against horizontal range for the flight test.
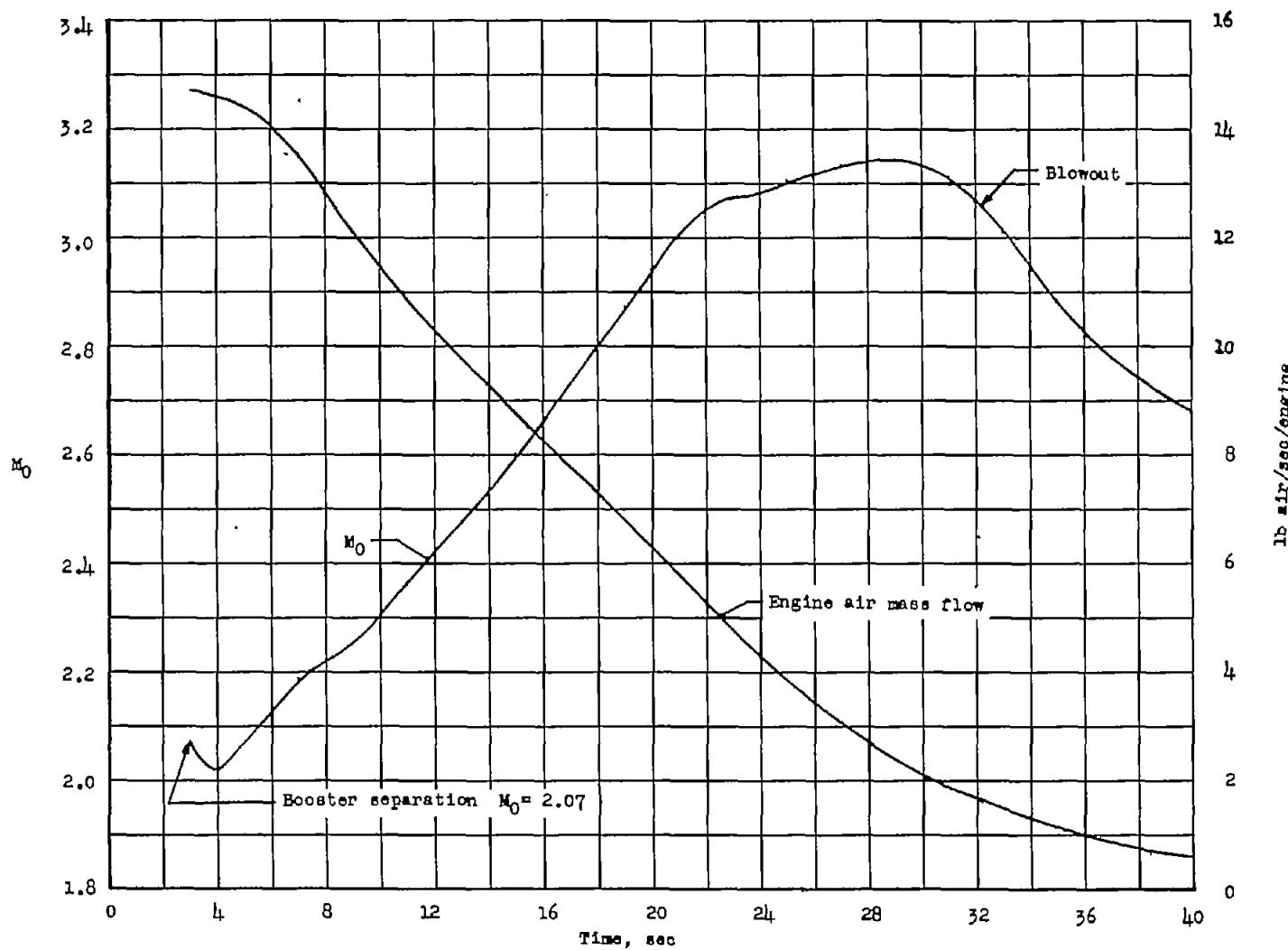
Figure 10.- Variation of Mach number and engine air rate with time for the flight test.
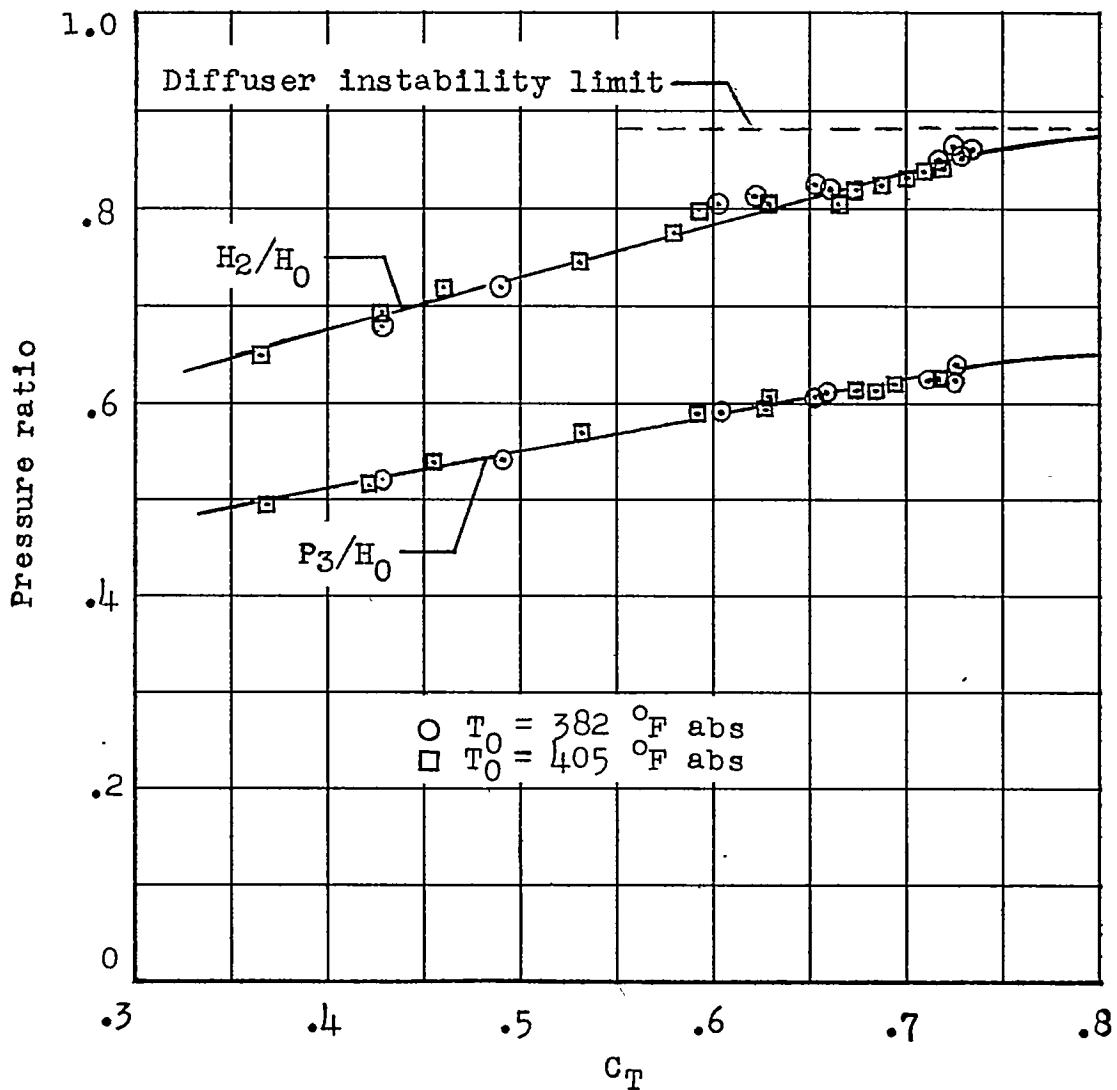
Figure 11.- Variation of engine total pressure and combustion-chamber pressure as a function of engine thrust coefficient for preflight tests at M = 1.84.
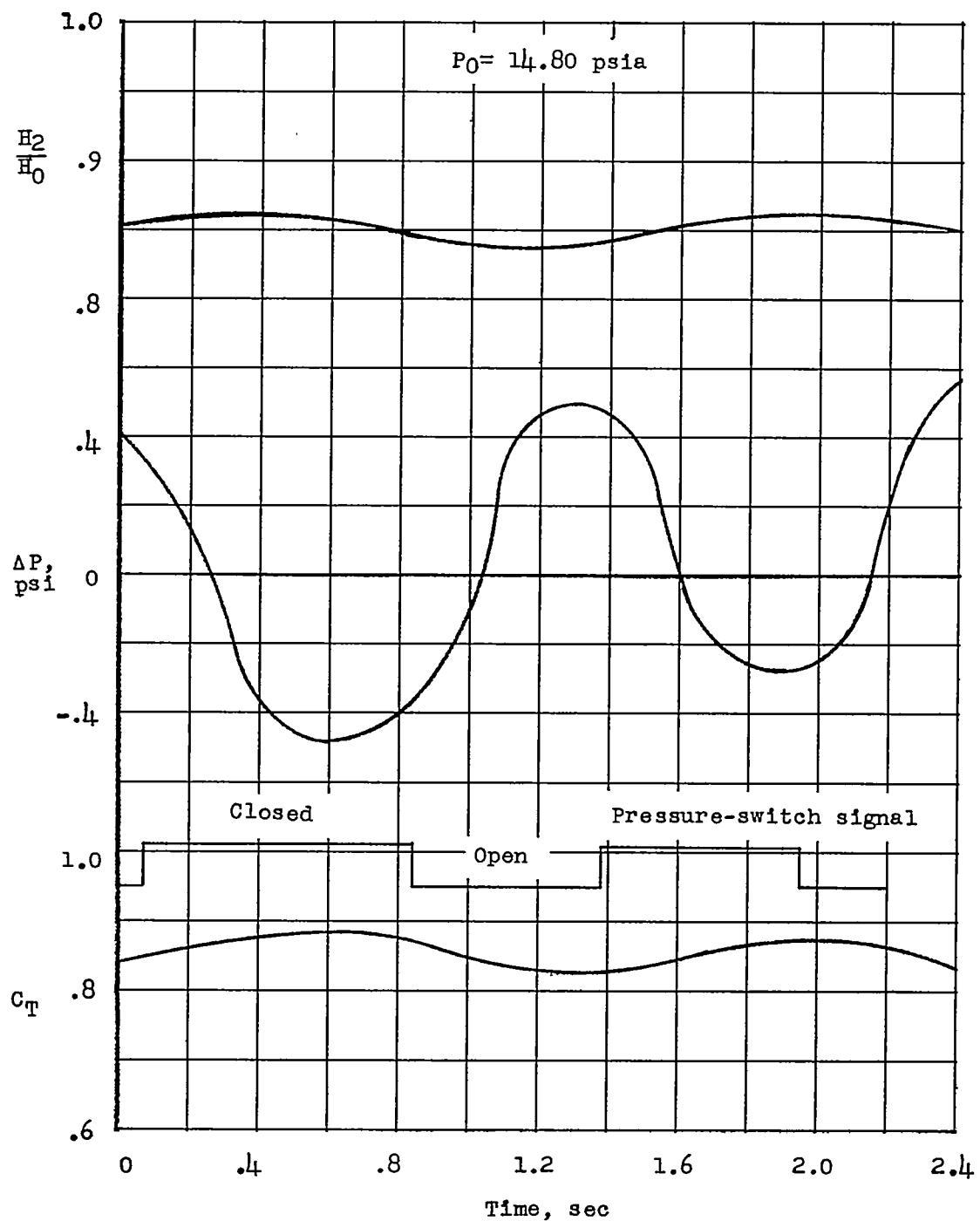
(a) Constant free-stream static pressure.

Figure 12.- Typical operating characteristics of thrust-coefficient control system with constant fuel pressure and density for M = 1.84 free-jet tests.
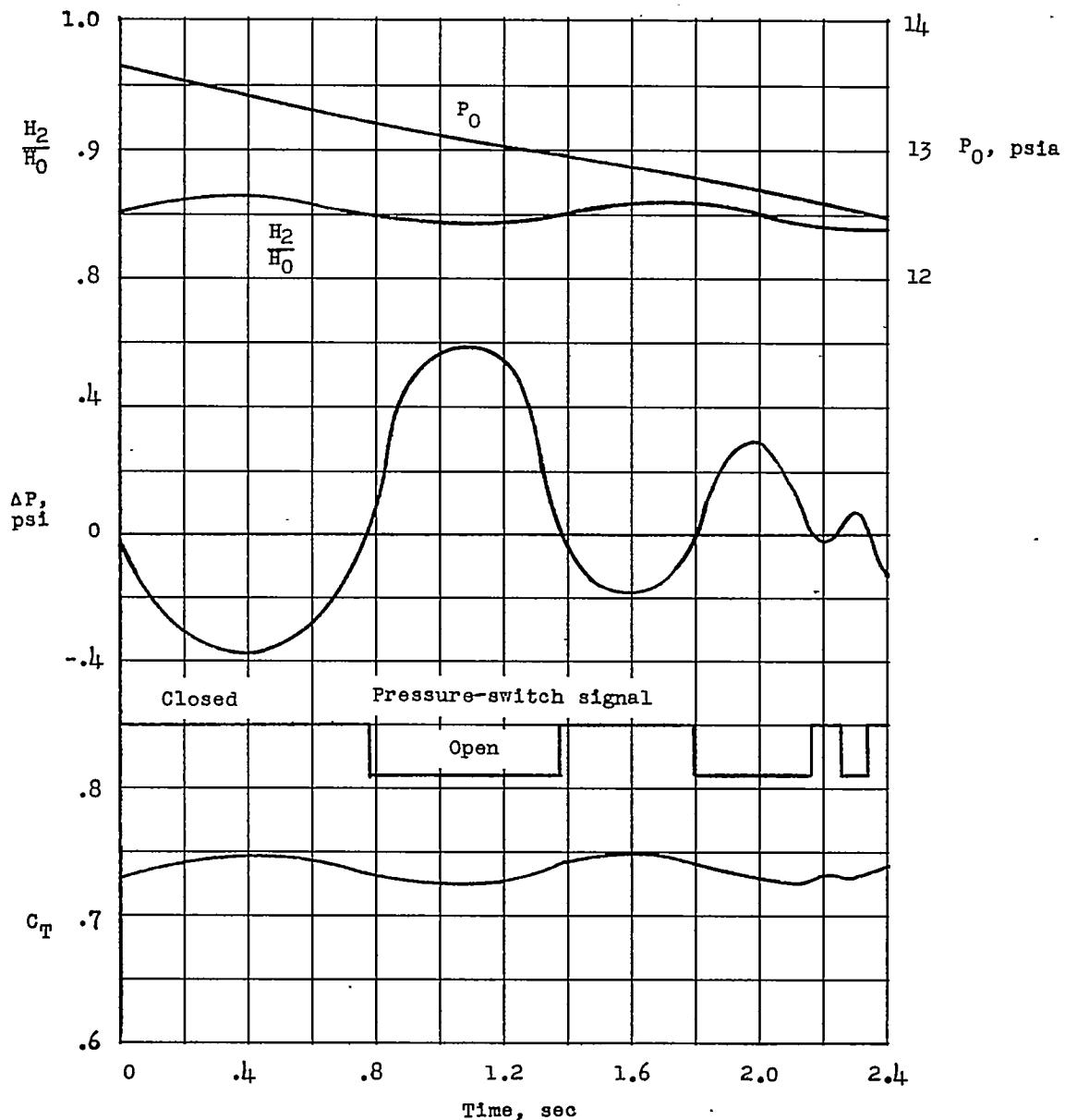
(b) Decreasing free-stream static pressure.

Figure 12.- Concluded.
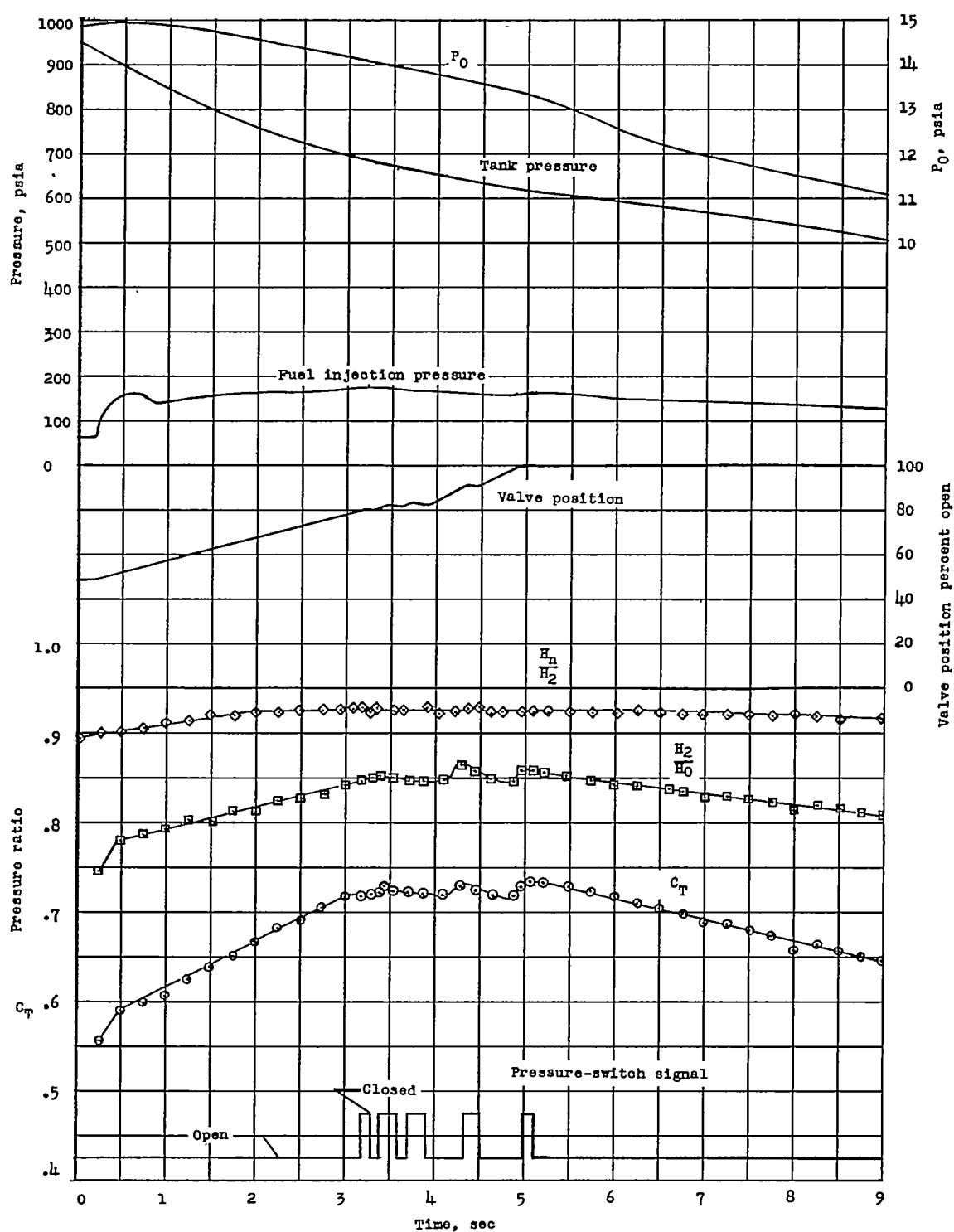
Figure 13.- Typical operating characteristics of the thrust-coefficient control system under simulated flight conditions in $M = 1.84$ free-jet tests.
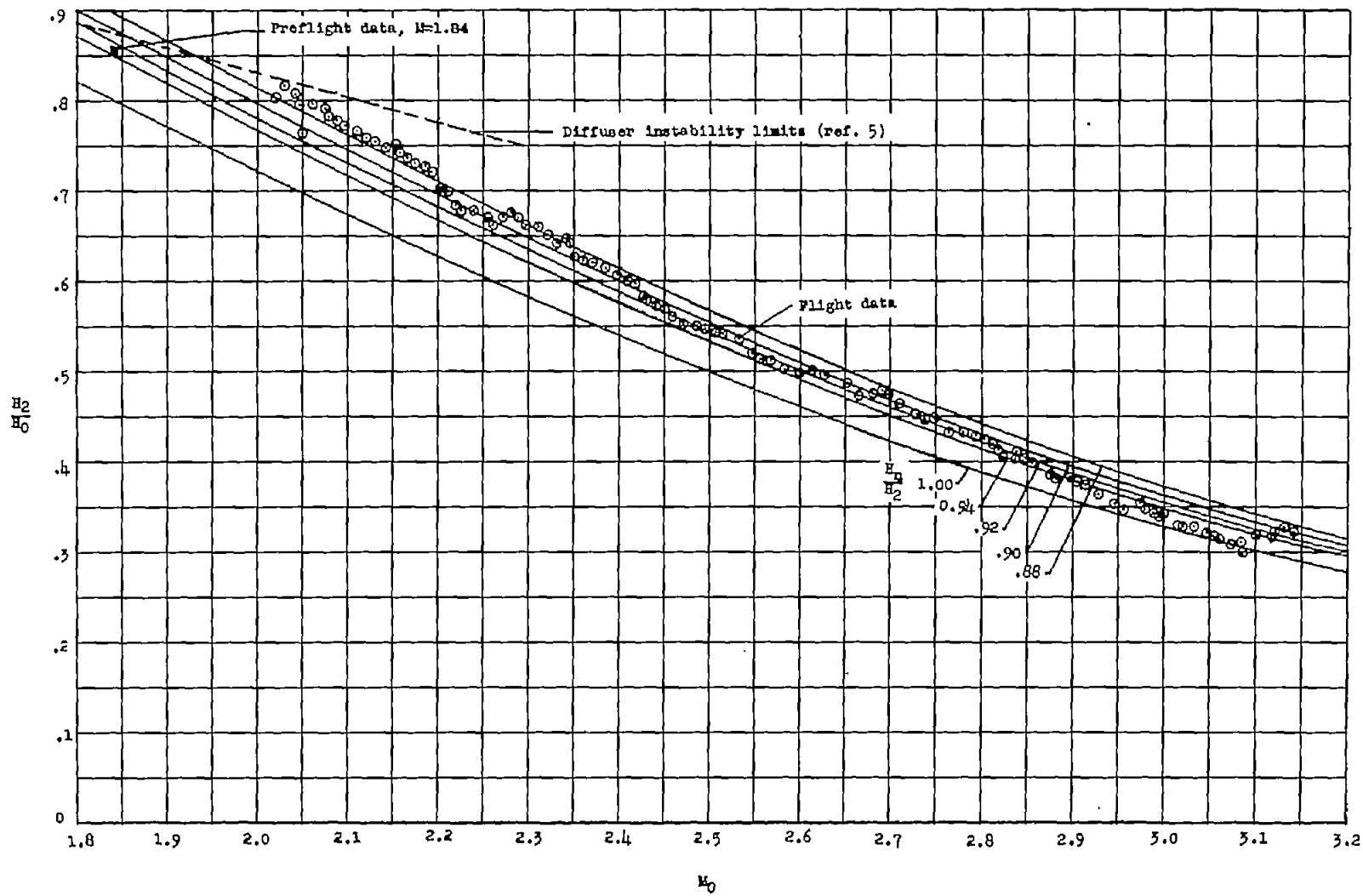
Figure 14.- Diffuser total pressure recovery plotted against Mach number for various control pressure ratios.
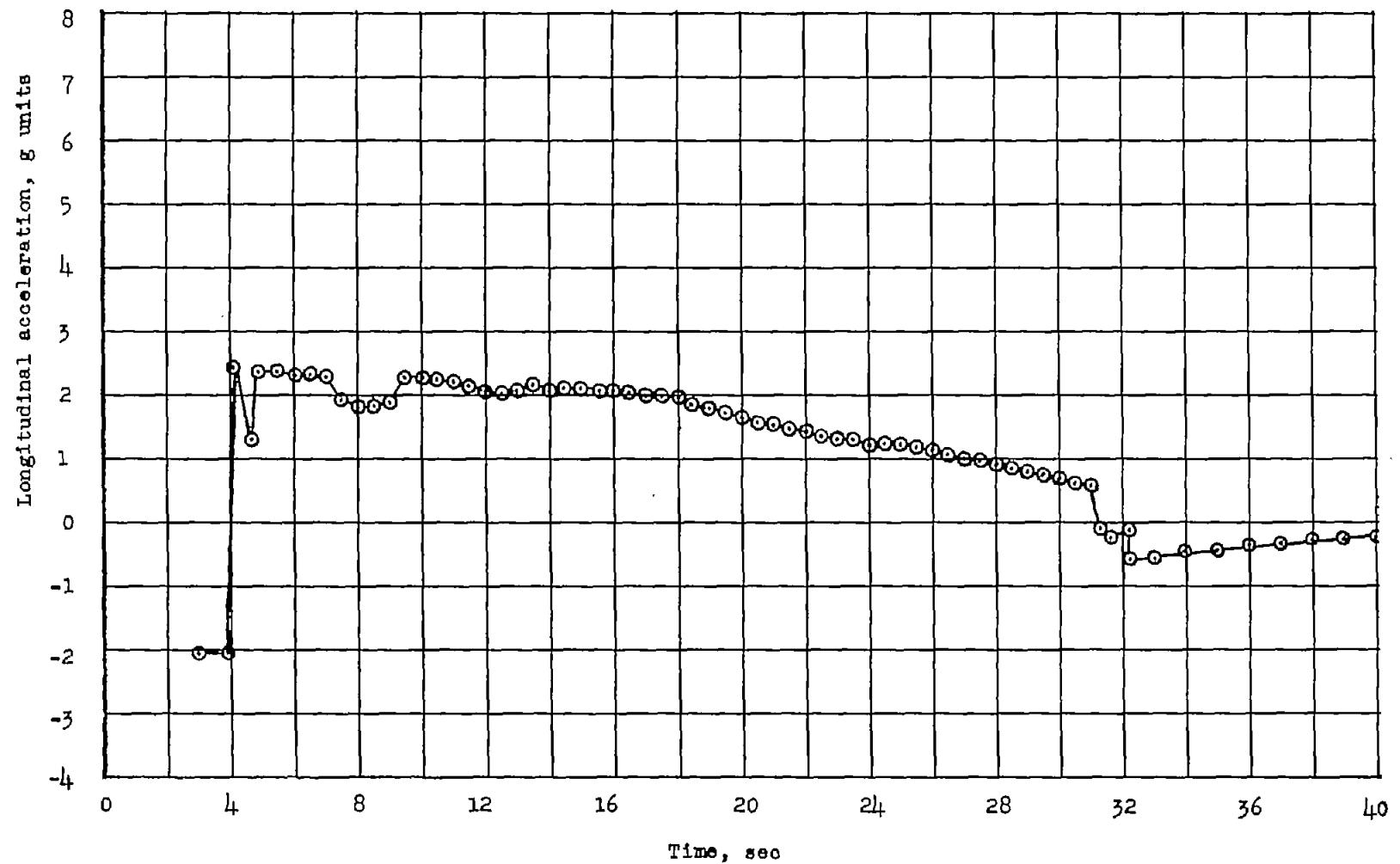
Figure 15.- Variation of acceleration with time for the flight test.
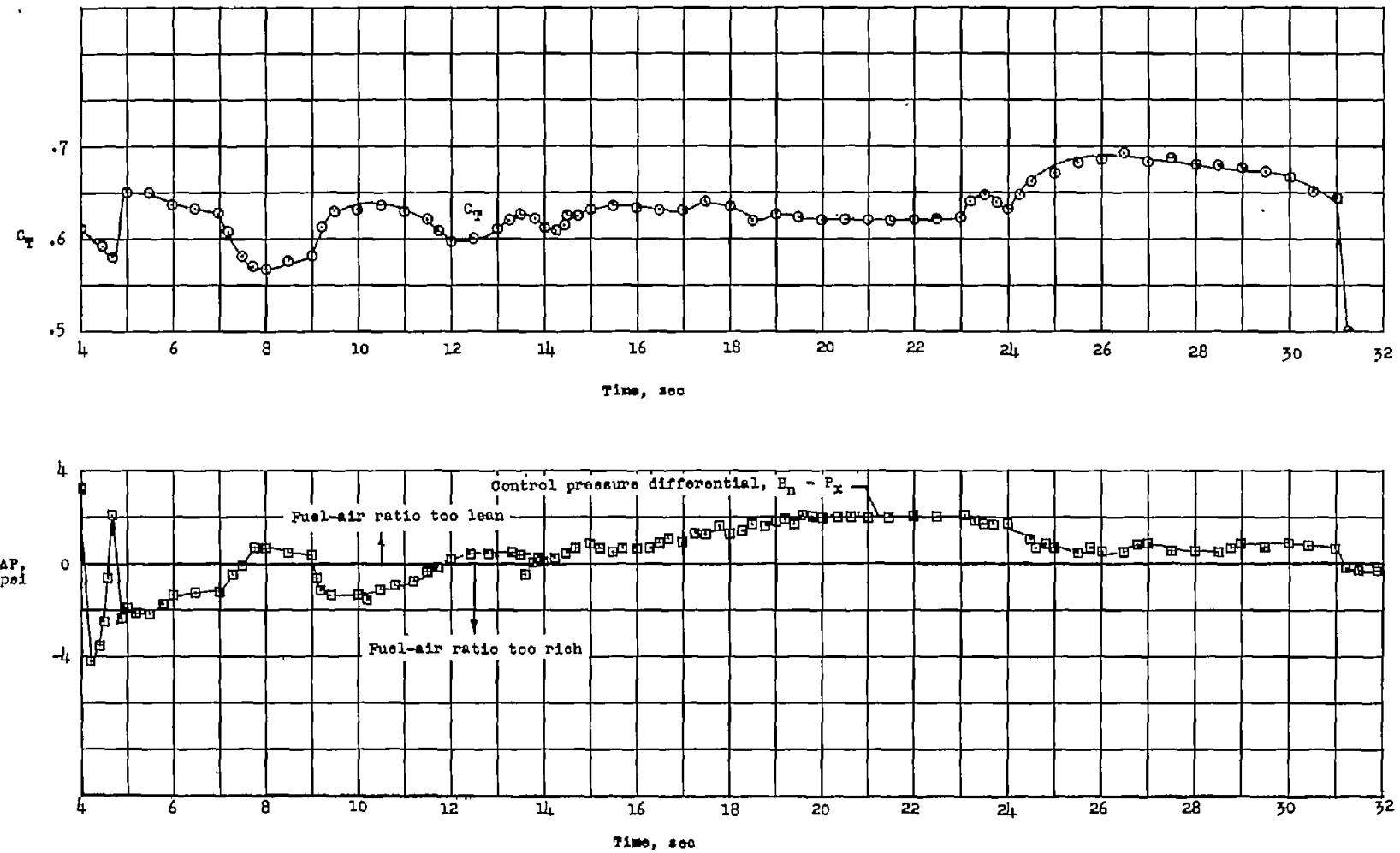
Figure 16.- Thrust coefficient and pressure switch differential plotted against time for flight test.
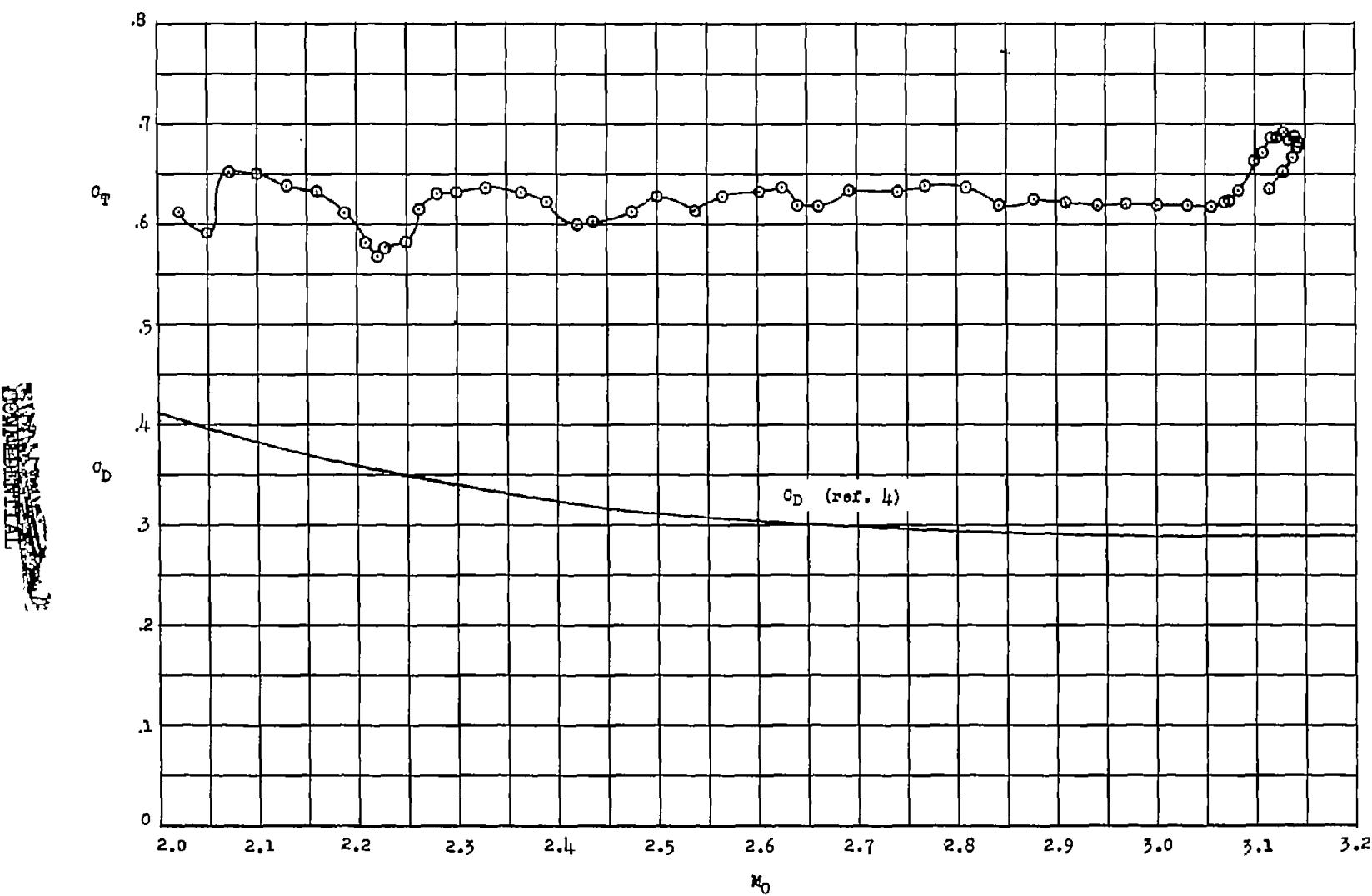
Figure 17.- Variation of thrust coefficient with Mach number for the flight
test and for various control pressure ratios.
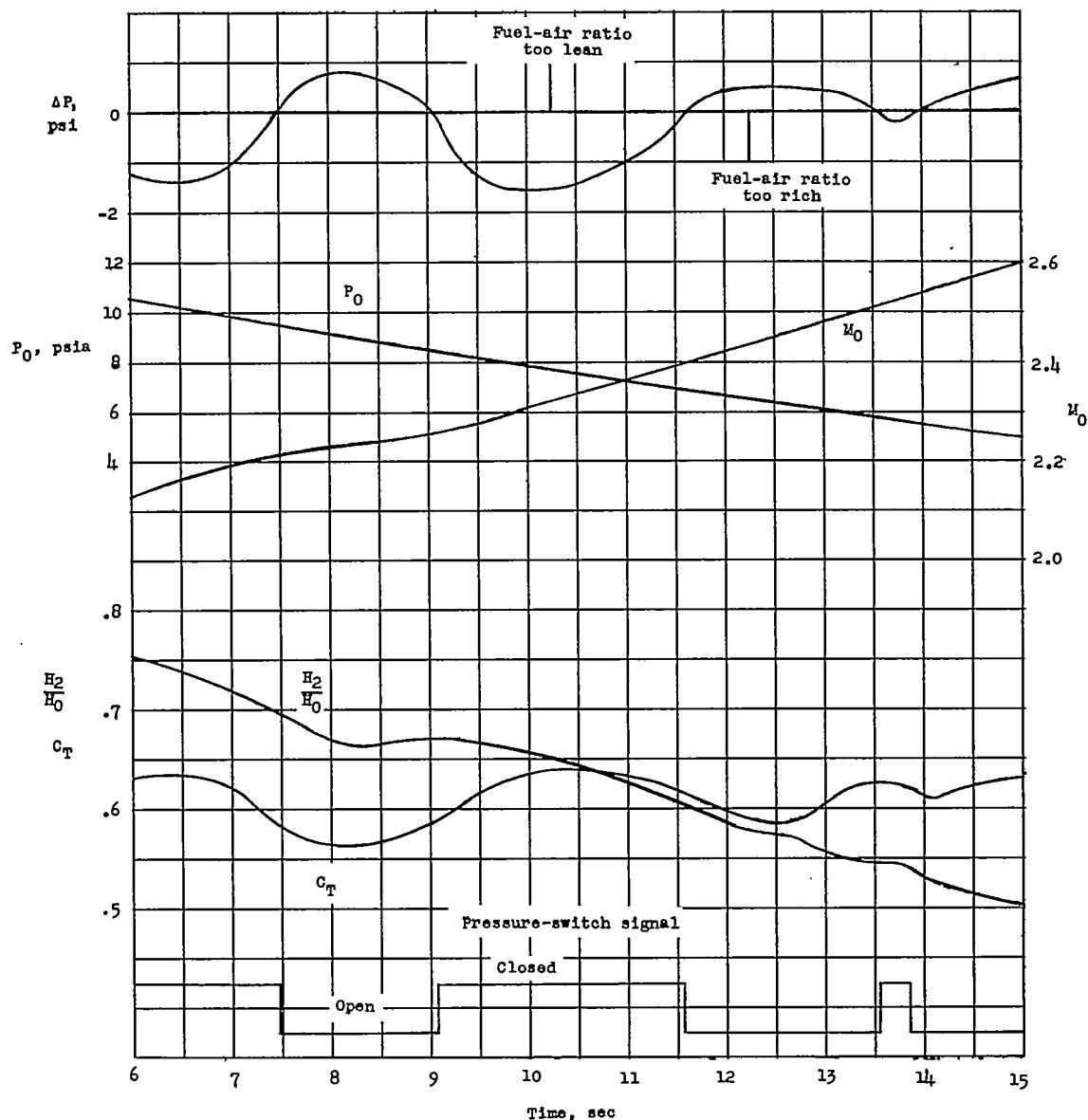
Figure 18.- Typical operating characteristics of the control system during the flight test.
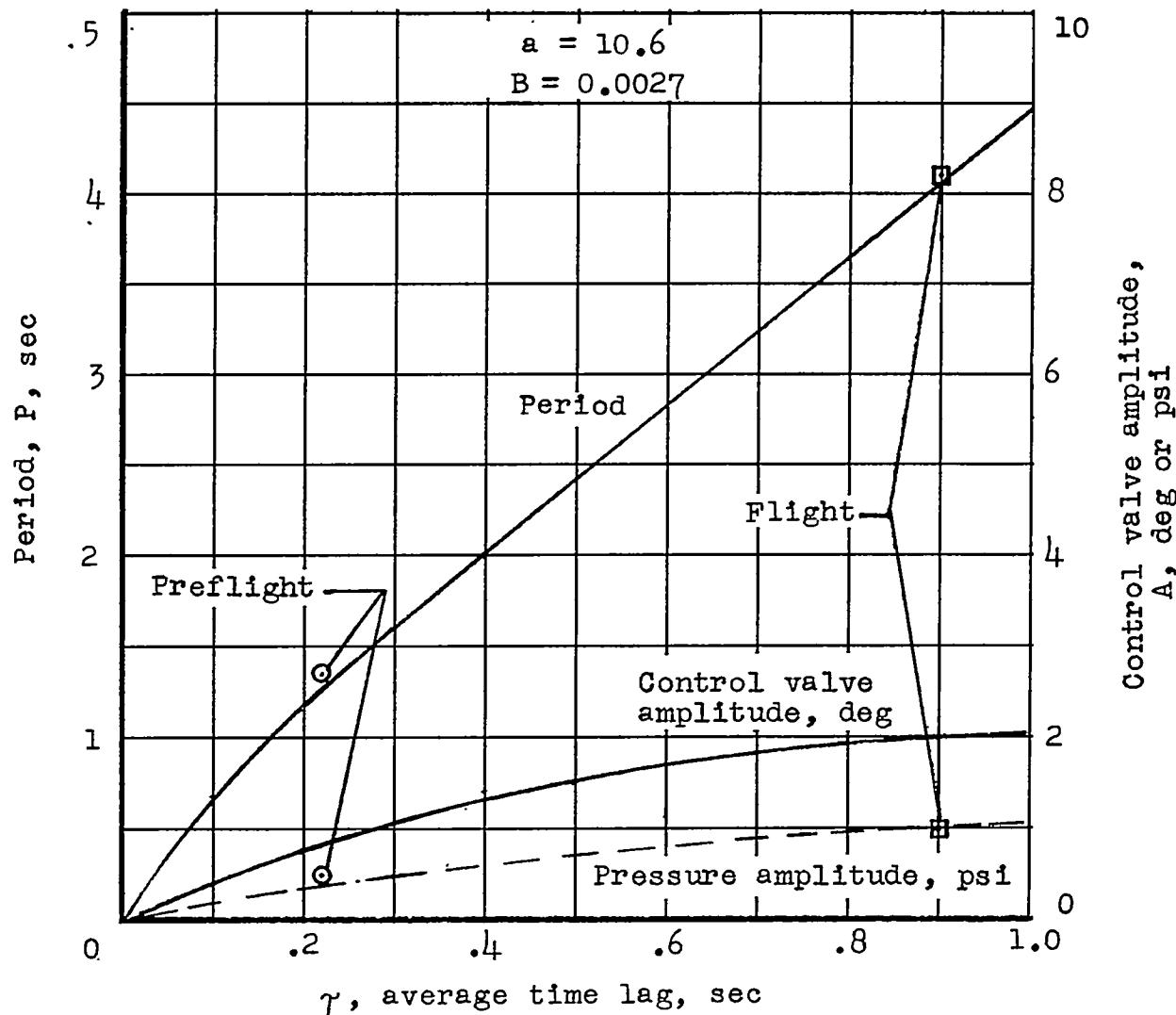
(a) Servo characteristics as a function of time lag.

Figure 19.- Servocontrol analysis.
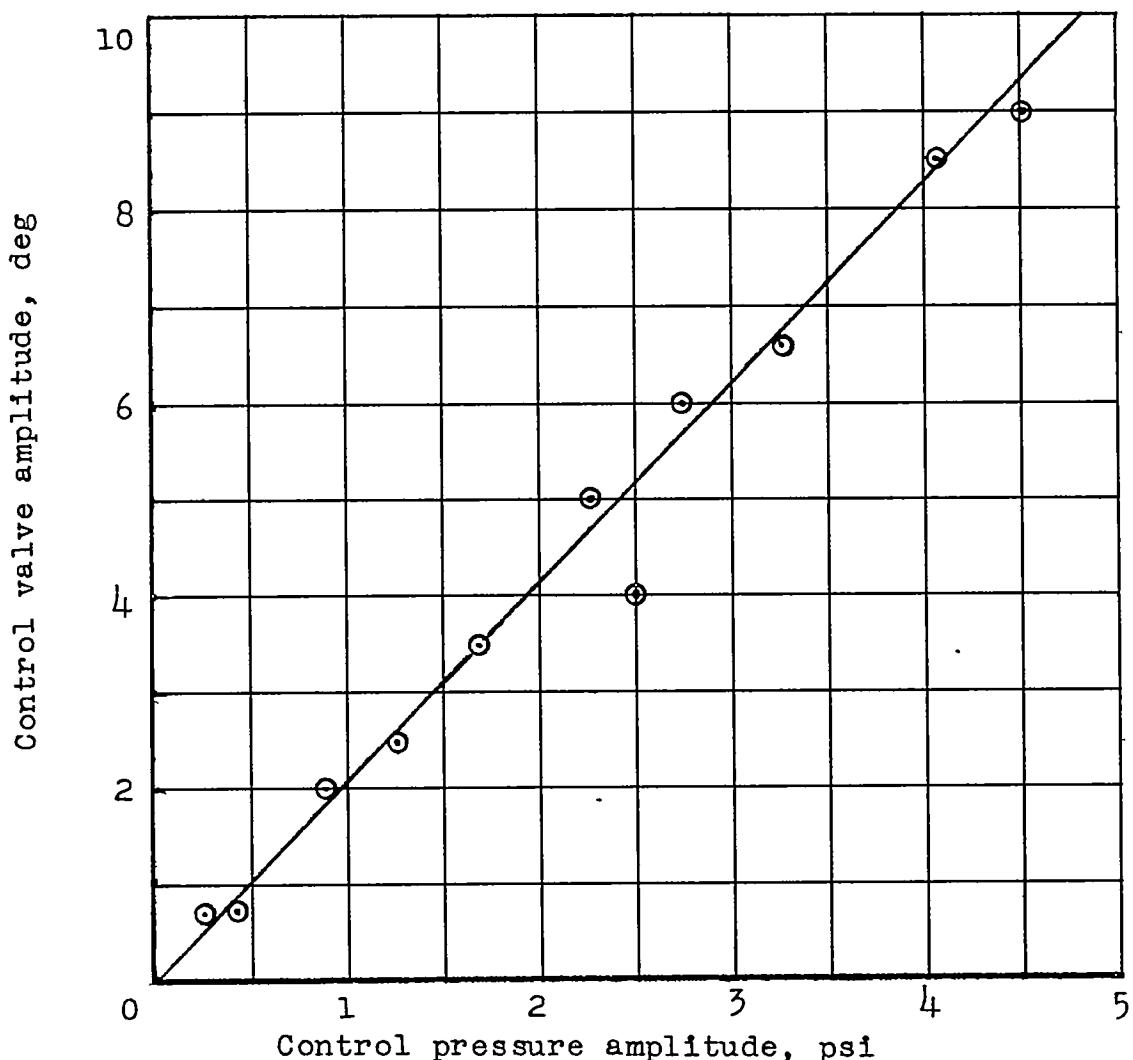
(b) Differential pressure control amplitude plotted against control valve amplitude as obtained in preflight tests.

Figure 19.- Concluded.